$7N-34$
$195451$
$47\%$

# NASA

# TECHNICAL NOTE

## D-53

EFFECT OF DISTRIBUTED THREE-DIMENSIONAL ROUGHNESS AND

SURFACE COOLING ON BOUNDARY-LAYER TRANSITION AND

LATERAL SPREAD OF TURBULENCE

AT SUPERSONIC SPEEDS

By Albert L. Braslow, Eugene C. Knox,
and Elmer A. Horton

Langley Research Center
Langley Field, Va.

## NATIONAL AERONAUTICS AND SPACE ADMINISTRATION

WASHINGTON                                    October 1959

NATIONAL AERONAUTICS AND SPACE ADMINISTRATION

TECHNICAL NOTE D-53

EFFECT OF DISTRIBUTED THREE-DIMENSIONAL ROUGHNESS AND

SURFACE COOLING ON BOUNDARY-LAYER TRANSITION AND

LATERAL SPREAD OF TURBULENCE

AT SUPERSONIC SPEEDS[1]

By Albert L. Braslow, Eugene C. Knox,
and Elmer A. Horton

SUMMARY

An investigation was made in the Langley 4- by 4-foot supersonic pressure tunnel at Mach numbers of 1.61 and 2.01 to determine (1) the effect of distributed roughness on boundary-layer transition with the model surface at adiabatic wall temperature and cooled and (2) the effect of surface cooling on the lateral spread of turbulence. Both distributed granular-type and single spherical roughness particles were used, and transition of the boundary layer was determined by hot-wire anemometers. The transition-triggering mechanism of the three-dimensional roughness at supersonic speeds appeared to be the same as that previously observed at subsonic speeds. In fact, the critical value of the roughness Reynolds number parameter $\sqrt{R_{k,t}}$ (that is, the value at which turbulent spots are initiated by the roughness) was found to be approximately the same at supersonic and subsonic speeds when complete local conditions at the top of the roughness, including density and viscosity, were considered in the formulation of the roughness Reynolds number. For three-dimensional roughness at a Reynolds number less than its critical value, the roughness introduced no disturbances of sufficient magnitude to influence transition. Surface cooling, although providing a theoretical increase in stability to small disturbances, did not increase to any important extent the value of the critical roughness Reynolds number for three-dimensional roughness particles. Cooling, therefore, because of its effect on the boundary-layer thickness, density, and viscosity actually promoted transition due to existing three-dimensional surface roughness for given Mach and Reynolds numbers. The measured lateral spread of turbulence in the boundary layer appeared to be unaffected by the increased laminar stability derived from the surface cooling.

[1]Supersedes NACA Research Memorandum L58A17 by Albert L. Braslow, 1958.

INTRODUCTION

A low-speed experimental investigation of the effect of distributed granular-type roughness on boundary-layer transition as reported in reference 1 indicated that, when the roughness is sufficiently submerged in the boundary layer to provide a substantially linear variation of local velocity with distance from the surface up to the top of the roughness, turbulent spots begin to appear immediately behind the roughness when a local roughness Reynolds number, based on the velocity at the top of the roughness and the roughness height, exceeds a critical value.

These data, as well as those of references 2 and 3, for example, indicate that, at roughness Reynolds numbers even slightly below the critical value, three-dimensional type of roughness introduces no disturbances of sufficient magnitude to influence transition but that only a very small increase of roughness Reynolds number above the critical value is required to move transition substantially up to the roughness. This mechanism of transition is in sharp contrast with experience with two-dimensional type of disturbances (for example, full-span cylindrical wires) where transition occurs some distance downstream of the roughness and gradually moves forward to the roughness position as the Reynolds number is increased. (See refs. 3 and 4.)

The purpose of the present tests was to extend the investigation of reference 1 to supersonic speeds to determine whether the transition-triggering mechanism of distributed three-dimensional particles is the same at supersonic speeds as that observed at subsonic speeds and to determine the critical value of the roughness Reynolds number at the higher speeds. In addition, information on the effects of increased laminar boundary-layer stability on boundary-layer transition associated with surface roughness and on the lateral spread of turbulent contamination behind a roughness particle was desired.

The investigation was made on a $10^\circ$ cone model and on a two-dimensional flat-plate model in the Langley 4- by 4-foot supersonic pressure tunnel at Mach numbers of 1.61 and 2.01. Various combinations of distributed roughness size and location were investigated on the cone; single particles of varying size and position were used on the flat-plate model in order to get a well-defined turbulence wedge. Both models were tested with the surfaces at adiabatic wall temperature and with the surfaces cooled. Indications of the nature of the boundary-layer flow were obtained by means of a hot-wire anemometer.

L
2
9
6

SYMBOLS

| | |
|---|---|
| $k$ | height of roughness particle |
| $L$ | characteristic length (most rearward roughness position), 12.5 in. |
| $M$ | Mach number |
| $R'$ | Reynolds number per foot based on flow outside boundary layer, $U/\nu_o$ |
| $R_k$ | Reynolds number based on roughness height and local flow conditions at top of roughness, $u_k k/\nu_k$ |
| $R_s$ | Reynolds number based on surface distance from leading edge and flow conditions outside boundary layer, $Us/\nu_o$ |
| $s$ | surface distance from leading edge to roughness |
| $T$ | local temperature, $^oR$ |
| $\bar{T}_w/T_o$ | ratio of average local temperature to local temperature outside boundary layer |
| $U$ | local streamwise component of velocity just outside boundary layer |
| $u$ | local streamwise component of velocity in boundary layer |
| $X^*$ | ratio of surface distance from leading edge to characteristic length, $s/L$ |
| $y$ | distance normal to surface |
| $\delta$ | boundary-layer total thickness |
| $\eta$ | nondimensional distance normal to surface, $(y/2s)\sqrt{R_s}$ |
| $\eta_k$ | nondimensional roughness height, $(k/2s)\sqrt{R_s}$ |
| $\nu$ | coefficient of kinematic viscosity |

Subscripts:

k       conditions at top of roughness particle

o       local conditions outside boundary layer

t       conditions at which turbulent spots appear

w       conditions at wall

$\infty$       conditions in undisturbed free stream

<div align="center">MODELS</div>

Two different configurations were used in the present investigation - a $10°$ cone and a two-dimensional flat plate. Actually two different models were used in the $10°$ cone test program: (1) a solid aluminum-alloy cone 24 inches long and (2) a hollow, thin-walled, stainless-steel cone $25\frac{1}{2}$ inches long for the cooling tests. Although the latter model was not the most desirable for the heat-transfer experiments because of its inability to attain a uniform longitudinal temperature distribution when cooled, it was used because of its availability and because it permitted attainment of valid effects of surface cooling on boundary-layer transition in the presence of surface roughness. Figure 1 includes a sketch of the hollow model and the locations of iron-constantan thermocouples used to measure the surface temperatures. A photograph of this model is presented as figure 2.

The flat-plate model which had a polished steel surface with a sharp leading edge was 48 inches wide and had a chord of 40 inches. The lower surface contour was approximately a segment of a circular arc. The model was hollow to permit surface cooling and was instrumented with iron-constantan thermocouples at known chordwise positions at the tunnel center line. The flat-plate surface was selected because of the ease of measurement of the lateral spread of turbulence on a flat surface. A photograph of the flat-plate model is presented as figure 3.

<div align="center">APPARATUS AND TESTS</div>

The investigation was made at Mach numbers of 1.61 and 2.01 in the Langley 4- by 4-foot supersonic pressure tunnel, which is a rectangular, closed-throat, single-return wind tunnel with provisions for control of

the air stagnation pressure, temperature, and humidity. The appearance of transition was observed by means of a hot-wire anemometer, the output of which was fed into an oscilloscope. The wire, which was a 3/32-inch length of 0.0003-inch-diameter tungsten, was arranged to be sensitive to variations in the u-component of velocity. For the $10^o$ cone models, three hot wires were located circumferentially $120^o$ apart approximately 6 inches from the base of the model in order to improve the probability of retaining a wire for the duration of a test run. These odds proved to be satisfactory because no runs were aborted as a result of the loss of all three wires, although at least one wire was lost each time. For the flat-plate model, a single hot wire, located 26.77 inches from the leading edge, was mounted on a spanwise traversing carriage. This arrangement permitted measurements of the velocity fluctuations at several spanwise positions during a single run. For tests of both the cone and flat-plate configurations, records of the hot-wire response to velocity fluctuations were made by photographing the traces on a cathode-ray tube.

Carborundum grit of various size, thinly spread over the surface in strips of about 3/16-inch width, was used as the distributed three-dimensional roughness on the $10^o$ cone. Closeup photographs of three representative strips are presented as figure 4. For each of the following investigated combinations of roughness size and location along the surface from the cone apex, the roughness was submerged in the boundary layer:

| Surface distance from cone apex, in. | Grit number | Mean grit height, in. | Maximum grit height present, in. |
|---|---|---|---|
| 1 | 180 | 0.0035 | 0.005 |
| 2 | 180 | .0035 | .005 |
| 2 | 80 | .0083 | .010 |
| 3 | 80 | .0083 | .010 |
| 3 | 70 | .0098 | .015 |
| 5 | 60 | .0117 | .023 |
| 5.9 | 240 | .0029 | .003 |
| 10.3 | 60 | .0117 | .023 |
| 10.4 | 80 | .0083 | .010 |
| 10.4 | 80 | .0083 | .011 |
| 12.5 | 60 | .0117 | .019 |

The height of the particles in each roughness strip tested was carefully measured with a 15-power shop microscope before and after each test run. The maximum height found is listed in the last column of the preceding table. Single three-dimensional roughness particles, which were actually steel miniature ball bearings, were used in the

flat-plate tests at various known positions on the surface and for all combinations used the roughness was well within the boundary layer. The height of the particles was carefully measured with the 15-power microscope after application to the surface.

The 10° cone model was cooled by means of liquid carbon dioxide which was sprayed into the interior of the hollow model through small orifices drilled in and near the end of a 1/4-inch-diameter copper tube. The tube was brought through the base of the model and was located approximately as indicated in figure 1. The cooling apparatus in the flat-plate model consisted of three 1/4-inch-diameter copper tubes with small holes drilled along the tube length. The chordwise spacing of the tubes was such as to concentrate most of the cooling in the region ahead of the 50-percent-chord location. The coolant, liquid carbon dioxide, was fed to the tubes by means of a manifold arrangement from a single bottle.

The test procedure during both phases of the investigation consisted of starting the tunnel at a low value of stagnation pressure and equivalent unit Reynolds number (Reynolds number per foot) and then gradually increasing the Reynolds number to values greater than those required for the initiation of turbulent spots behind the roughness. Photographs of the hot-wire response were taken for various types of boundary-layer flow throughout the stagnation-pressure range. For the cooling tests of the cone, the model was cooled after the unit Reynolds number was adjusted to the critical point, that is, the stagnation pressure at which turbulent spots began to appear. Photographs of the change in boundary-layer character were made and then the stagnation pressure readjusted to return the flow to the almost completely laminar condition (that is, with the occurrence of spots) at which point photographs were again taken. For determination of the effect of surface cooling on the lateral spread of turbulence on the flat plate, the unit Reynolds number was increased to a value at which the hot-wire response indicated 100-percent turbulent flow directly behind the roughness. The time variation of turbulence as a function of spanwise position was then recorded for the model surface both at adiabatic wall and cooled temperatures. The distribution of surface temperature for both models was recorded simultaneously on Brown potentiometers and a direct correlation was kept between the oscillograph photographs, potentiometer records, and tunnel stagnation pressure and temperature. For large amounts of cooling, frost formations on the model surface initiated occurrence of turbulent spots and in some cases resulted in wire breakage, probably because of collision of ice particles with the hot wire. The data presented have been limited to frost-free conditions.

Some secondary test points were taken for which the roughness particles were very close to the leading edge of the model and the height of the roughness was approximately equal to the boundary-layer total thickness. This limited amount of data was taken in order to establish some

indication of the change, if any, in the critical roughness Reynolds number when the roughness height is equal to or greater than the boundary-layer total thickness. The test procedure for these runs was similar to that previously discussed except that data were taken only for equilibrium conditions.

## RESULTS AND DISCUSSION

### Interpretation of Data

A representative example of the various types of boundary-layer flow observed is given in figure 5 in the form of hot-wire traces of the time variation of velocity in the boundary layer. On the vertical scale of the figure is given the value of tunnel unit Reynolds number corresponding to each trace. Shown at the top of the figure is the time scale for the traces. Time increases from left to right. The amplifier and oscillograph attenuations were maintained the same for all hot-wire traces taken during each test run. The trace at a unit Reynolds number of $0.86 \times 10^6$ denotes laminar flow. Infrequent disturbances of very short duration were initiated at a unit Reynolds number of $0.90 \times 10^6$. These disturbances increased in frequency with a further increase in Reynolds number until, at a unit Reynolds number of $0.974 \times 10^6$, the flow was completely turbulent. For a smooth model, natural transition would not have progressed past the measuring station through the test Reynolds number range of figure 5. These observed changes in the character of the boundary layer with changes in Reynolds number are similar to those observed at subsonic speeds in reference 1 and are consistent with the concept of the origin of turbulence as turbulent spots that grow in size as they move downstream. (See ref. 5.)

The hot-wire traces of figure 6 also verify the indications of references 1 to 3 that, for three-dimensional roughness at a Reynolds number less than its critical value, the roughness will introduce no disturbances of sufficient magnitude to influence transition. At a unit Reynolds number of $2.86 \times 10^6$, the flow was laminar for both the model in the smooth condition and the model with 0.003-inch roughness located 5.9 inches from the cone apex. At a unit Reynolds number of $3.29 \times 10^6$, infrequent turbulent spots appeared at the hot-wire location for both model surface conditions, and an increase in the unit Reynolds number increased the frequency of occurrence of the spots until the flow was almost completely turbulent at a unit Reynolds number of about $4.0 \times 10^6$.

Although for the same or slightly lower values of the unit Reynolds number the turbulent spots appear to occur somewhat more frequently for the rough-surface condition than for the smooth condition, the differences involved are associated with such small increments in Reynolds number within the range required to change the flow from the initial formation of spots to the fully turbulent condition that it appears highly improbable that a repeated test for either surface condition could duplicate the comparisons to such a degree of accuracy. In fact, these differences are of the same order of magnitude as typical scatter in other experimental investigations of transition such as found in reference 6. If the roughness applied to the model for the test of figure 6 had introduced significant disturbances into the laminar layer, transition would have occurred at the hot-wire location at an appreciably lower value of the Reynolds number than that required to move transition forward of that point with the model smooth $\left(3.3 \times 10^6 < R' < 4.0 \times 10^6\right)$. On the basis of the roughness correlation presented in a later section, a roughness height of 0.007 to 0.008 inch is required to promote premature transition for the test conditions of figure 6.

### Correlation of Data

Correlation of boundary-layer transition due to a randomly distributed three-dimensional type of surface roughness has been accomplished at subsonic speeds in reference 1 on the basis of a critical local roughness Reynolds number formulated with the velocity at the top of the roughness and with the roughness height. That such a roughness Reynolds number should afford a basis for correlation is founded on the concept that, for geometrically similar projections submerged in the linear portion of the variation of boundary-layer velocity with distance from the surface, discrete disturbances form at the roughness particles when the local Reynolds number of the flow about the roughness reaches a critical value. The critical value of this roughness Reynolds number for the roughness of reference 1 was found to be approximately 600.

The square root of the roughness Reynolds number was chosen in the present investigation as the variable inasmuch as the value $\sqrt{R_{k,t}}$ is more nearly proportional to the critical projection height than $R_{k,t}$ for the projection submerged in the linear portion of the boundary-layer velocity profile. At supersonic speeds, where a variation of density and viscosity as well as velocity exists through the boundary layer, the exponent of $R_{k,t}$ for linearity with $k$ is even smaller than $1/2$. In order to consider the effect of Mach number on the boundary-layer density and viscosity, the values of the roughness parameter $\sqrt{R_{k,t}}$ for the supersonic results were obtained with the use of kinematic

viscosity based on conditions at the top of the projection as well as the height of the projection and the velocity at the particle height. The maximum measured height of the particles in each roughness strip on the $10^\circ$ cone (as presented in the table in "Apparatus and Tests") and the measured height of the single roughness particles on the flat plate were used in the calculation of the critical roughness Reynolds number. The velocity and temperature distributions through the boundary layer used in the computation of $\sqrt{R_{k,t}}$ were calculated for the flat plate by the methods of reference 7 and for the cone by correcting the flat-plate calculations to the cone conditions by Mangler's transformation. Representative temperature and velocity profiles for the cone are presented in figures 7 and 8 for adiabatic wall conditions at surface Mach numbers of 1.58 and 1.95 corresponding to undisturbed free-stream Mach numbers of 1.61 and 2.01, respectively.

## Critical $R_{k,t}$ Value

The results of the present investigation at supersonic speeds for the flat-plate and the cone surfaces at adiabatic wall temperature are summarized in figure 9(a) in the form of a plot of $\sqrt{R_{k,t}}$ against roughness location for the various roughness sizes tested. It is apparent from this figure that approximately the same values of the roughness parameter $\sqrt{R_{k,t}}$ as determined in reference 1 can be used, for practical purposes, to predict the initiation of turbulence caused by distributed three-dimensional roughness at supersonic speeds at least up to a Mach number of 2 when the value of $\sqrt{R_{k,t}}$ is based on the local density and viscosity as well as on the local velocity at the roughness height. It seems reasonable to expect that the same transition phenomenon and approximate critical value of roughness Reynolds number would be applicable for further moderate increases in the value of supersonic Mach number although a sparse amount of information in reference 8 indicates an increase in $\sqrt{R_{k,t}}$ at Mach numbers of 5 to 7. Additional experimentation is needed to verify this trend.

It is worthwhile at this point to focus attention on the interval in unit Reynolds number between the value at which turbulent bursts are first initiated at the roughness and that at which a fully developed turbulent boundary layer exists in the immediate vicinity of the roughness. The latter case, of course, is important in determination of the conditions for which turbulent heat-transfer and skin-friction characteristics are obtained. Reference 1 indicates that at subsonic speeds this interval in Reynolds number is small; however, at supersonic speeds

some information has been obtained that indicates a larger interval in Reynolds number. More research is required to clarify this possibility.

## Effect of Surface Cooling on Critical $R_{k,t}$ Value

It is well known from the theories of amplification of small disturbances in a laminar boundary layer that, for a stable laminar layer, small two- or three-dimensional disturbances will damp out as they move downstream. It is also known that either boundary-layer suction or cooling has a stabilizing effect on the laminar layer for these theoretically small disturbances. Depending upon the amount of suction (ref. 9, for example) or cooling (refs. 10 to 13), then, the transition Reynolds number based on the extent of laminar flow can be appreciably increased over the natural transition Reynolds number if the surfaces are sufficiently devoid of either three-dimensional or two-dimensional types of roughness elements. For two-dimensional roughness elements of finite size, it has been found that cooling can have a beneficial stabilizing effect in that some increase in transition Reynolds number can be obtained depending upon the value of Mach number, the size of the two-dimensional roughness, and the amount of cooling. (See ref. 12.) For three-dimensional roughness elements of finite size, however, reference 14 indicated that at subsonic speeds, at least, the critical value of the three-dimensional roughness Reynolds number was not greatly increased when the boundary layer was stabilized through application of continuous suction. This difference in the effect of laminar boundary-layer stability on the initiation of turbulence caused by two- or three-dimensional type of roughness is associated with the basic difference in the triggering mechanism of turbulence that has been experimentally determined for the two types of roughness as previously described. That is, disturbances resulting from two-dimensional roughness appear to be of the Tollmien-Schlichting type and are subject to amplification theories whereas disturbances resulting from three-dimensional roughness, on the basis of low-speed experimentation, do not appear to be subject to such stability arguments.

The effect of surface cooling in the presence of roughness on boundary-layer transition at supersonic speeds is shown in figure 10 by a comparison of the hot-wire traces observed for the cone surfaces at adiabatic wall temperature and for the cone surfaces cooled. It was clearly demonstrated that, when the roughness Reynolds number was just critical $\left(R' \approx 1.18 \times 10^6\right)$, that is, when turbulent spots began to appear with the surface at adiabatic wall temperature, cooling the cone surface resulted in a completely turbulent boundary layer. In fact, for the cooled condition it was necessary to decrease appreciably the tunnel unit Reynolds number in order to return the boundary layer to the laminar condition. Associated with the surface cooling for given values of

roughness size, free-stream Reynolds number, and Mach number is an increase in roughness Reynolds number $R_k$ caused by an increase in velocity at the top of the particle (due to a thinning of the boundary layer and an increase in convexity of the velocity profile) as well as an increase in local density and a decrease in local viscosity both of which are due to the lowered boundary-layer temperature. These effects of surface cooling on the local velocity and temperature distributions are shown by comparison of figures 11(a) and 12(a) for cooled surfaces with figures 7 and 8 for surfaces at adiabatic wall temperature. Shown in figures 11(b) and 12(b) are representative experimental longitudinal surface-temperature distributions used in the calculations of the velocity and temperature profiles for the cooled case. As suggested in reference 7, polynomial expressions approximating the longitudinal temperature distributions were used in the aforementioned calculations.

The fact that transition resulted from the increase in roughness Reynolds number indicates that the critical value of roughness Reynolds number was not increased to any important extent by the theoretical increase in laminar boundary-layer stability to small disturbances resulting from the surface cooling. This conclusion is verified by the close agreement in the values of $\sqrt{R_{k,t}}$ presented in figure 9 for the cooled cone model and for both the cone and flat-plate models with the surface at adiabatic wall temperature and is consistent with reference 14 where it was shown that a laminar boundary layer made stable to vanishingly small disturbances by means of continuous suction was less sensitive to the finite three-dimensional type of surface disturbance only to a minor degree. Increased stability as obtained by a highly favorable pressure gradient over the forward portion of a sphere also yielded similar values of $\sqrt{R_{k,t}}$. (See ref. 15.) The present results also offer a most plausible explanation for the reversal in the trend of increasing transition Reynolds number with increased cooling that was noted in references 10, 13, and 16.

### Effect of Surface Cooling on Lateral Turbulent Spread

The effect of surface cooling on the lateral spread of turbulence in the boundary layer is shown in figure 13 by a comparison of the hot-wire traces observed for the flat-plate surface at adiabatic wall temperature and cooled. The ordinate of the figure shows the distance to the left or right of the roughness at which the measurement was made; the chordwise location of the measurement was 26.77 inches from the leading edge. The hot-wire trace taken directly behind the roughness (fig. 13(a)) shows the boundary layer to be turbulent 100 percent of the time, and the traces taken at several stations to the left and

right of the roughness indicate a progressive decrease in turbulence until fully laminar flow is obtained at the outer edge of the turbulent wedge. The differences in amplitudes of the hot-wire traces as the wire traverses the completely turbulent and intermittently turbulent regions are associated with the effect on the hot-wire cooling of the sudden changes in the mean velocity as the boundary layer varies between turbulent and laminar flow in addition to the effect of fluctuation of the turbulent velocity. The magnitude of the mean-velocity effect, of course, is dependent on the degree of submersion of the hot wire within the boundary layer. Comparison of the results for the adiabatic wall and the cooled wall flat plate at a Mach number of either 1.61 or 2.01 indicates that the lateral spread of the turbulence at the measuring station was not significantly decreased by the increased boundary-layer stability derived from the surface cooling. This result is more easily seen in figure 14 where the percentage of the time that turbulence was observed at each spanwise station, as estimated from figure 13, is plotted against the spanwise distance from the roughness at the measuring station.

Inasmuch as these measurements were made at a Reynolds number significantly greater than the critical value for the roughness, it is likely that the turbulent wedge was initiated near the roughness particles and that the sides of the wedge were straight. (See ref. 5.) Plan views of the turbulent wedges based on this assumption are also presented in figure 14 to provide an indication of the magnitude of the included angles for 100-percent turbulence and 0-percent turbulence. In the region outside the boundaries of the 0-percent turbulence, the flow is laminar; between the 0-percent and 100-percent boundaries, the flow is intermittently laminar and turbulent; and between the 100-percent turbulence boundaries, the flow is turbulent all the time. For adiabatic wall temperature conditions, the results indicate about the same values of wedge angle at a Mach number of 1.61 as those measured at low speeds (ref. 5) but show a reduction in wedge angle with an increase in Mach number to 2.01. A further decrease in the lateral spread of turbulence at a Mach number of 5.8 was shown in reference 17 as well as a slowly increasing angle of spread in the vicinity of the initial transition. Further detailed measurements of the spread of turbulence behind three-dimensional roughness particles at supersonic speeds would be desirable.

## Critical $R_{k,t}$ Value for $k = \delta$

Some of the runs on the flat plate were made with roughness of such a size and location that the roughness height was very near or equal to the boundary-layer total thickness. For these conditions the critical roughness Reynolds numbers were determined and are presented in figure 9. The ratio of the roughness height to the boundary-layer

total thickness for all the adiabatic wall data points of figure 9 may be obtained from figure 15. The nondimensional roughness height at the corresponding surface station for a given test point is determined from the plots of $\eta_{k,t}$ against surface distance from the model leading edge; the nondimensional boundary-layer total thickness is obtained from the velocity profiles presented in figure 15.

The values of the critical roughness Reynolds number of figure 9 for the roughness near the edge of the boundary layer appear to be somewhat larger than the values for which the roughness was submerged in the boundary layer. These results are consistent with those of reference 1 for roughness heights equal to and slightly greater than the boundary-layer total thickness. It should be recalled, however, that the conditions upon which the formulation of the roughness Reynolds number is based are violated when the roughness protrudes a significant amount beyond the linear portion of the velocity distribution.

The pertinent data used to calculate the values of $\sqrt{R_{k,t}}$ presented in figure 9 are presented in table I for both the 10° cone and the flat-plate models.

<div align="center">CONCLUSIONS</div>

An investigation made in the Langley 4- by 4-foot supersonic pressure tunnel at Mach numbers of 1.61 and 2.01 to determine the effect of distributed three-dimensional roughness and surface cooling on boundary-layer transition and the lateral spread of turbulence indicates the following conclusions:

1. The transition-triggering mechanism of distributed three-dimensional particles appeared to be the same at supersonic speeds as that previously observed at subsonic speeds.

2. The value of the three-dimensional roughness Reynolds number parameter $\sqrt{R_{k,t}}$ at which turbulent spots begin to appear behind the roughness was approximately the same at supersonic and subsonic speeds when the roughness Reynolds number is based on the local values of density, viscosity, and velocity at the top of the roughness and the roughness height.

3. For three-dimensional roughness with a Reynolds number less than its critical value, the roughness introduced no disturbances of sufficient magnitude to influence transition.

4. The critical three-dimensional roughness Reynolds number was not increased to any important extent by increasing the laminar boundary-layer stability to small disturbances through the use of surface cooling. For a given stream Mach number and Reynolds number, then, surface cooling will promote rather than delay transition due to existing three-dimensional roughness inasmuch as the actual value of roughness Reynolds number is increased by the effect of cooling on boundary-layer thickness, density, and viscosity.

5. The lateral extent of turbulence at a position approximately 19 inches downstream of a three-dimensional roughness particle was not significantly decreased by increasing the laminar boundary-layer stability through the use of surface cooling.

6. For the two test Mach numbers, the lateral extent of turbulence at the measuring station appeared to decrease with increasing Mach number.

7. The critical roughness Reynolds number for roughness nearly equal to the boundary-layer total thickness appeared to be somewhat larger than that for which the roughness is well submerged in the boundary layer.


Langley Research Center,
    National Aeronautics and Space Administration,
        Langley Field, Va., July 13, 1959.

L
2
9
6

REFERENCES

1. Von Doenhoff, Albert E., and Horton, Elmer A.:  A Low-Speed Experimental Investigation of the Effect of a Sandpaper Type of Roughness on Boundary-Layer Transition.  NACA Rep. 1349, 1958.  (Supersedes NACA TN 3858.)

2. Loftin, Laurence K., Jr.:  Effects of Specific Types of Surface Roughness on Boundary-Layer Transition.  NACA WR L-48, 1946. (Formerly NACA ACR L5J29a.)

3. Klebanoff, P. S., Schubauer, G. B., and Tidstrom, K. D.:  Measurements of the Effect of Two-Dimensional and Three-Dimensional Roughness Elements on Boundary-Layer Transition.  Jour. Aero. Sci. (Readers' Forum), vol. 22, no. 11, Nov. 1955, pp. 803-804.

4. Dryden, Hugh L.:  Review of Published Data on the Effect of Roughness on Transition From Laminar to Turbulent Flow.  Jour. Aero. Sci., vol. 20, no. 7, July 1953, pp. 477-482.

5. Schubauer, G. B., and Klebanoff, P. S.:  Contributions on the Mechanics of Boundary-Layer Transition.  NACA Rep. 1289, 1956.  (Supersedes NACA TN 3489.)

6. Schubauer, G. B., and Skramstad, H. K.:  Laminar-Boundary-Layer Oscillations and Transition on a Flat Plate.  NACA Rep. 909, 1948.

7. Chapman, Dean R., and Rubesin, Morris W.:  Temperature and Velocity Profiles in the Compressible Laminar Boundary Layer With Arbitrary Distribution of Surface Temperature.  Jour. Aero. Sci., vol. 16, no. 9, Sept. 1949, pp. 547-565.

8. Jedlicka, James R., Wilkins, Max E., and Seiff, Alvin:  Experimental Determination of Boundary-Layer Transition on a Body of Revolution at  M = 3.5.  NACA TN 3342, 1954.

9. Braslow, Albert L., Burrows, Dale L., Tetervin, Neal, and Visconti, Fioravante:  Experimental and Theoretical Studies of Area Suction for the Control of the Laminar Boundary Layer on an NACA 64A010 Airfoil.  NACA Rep. 1025, 1951.  (Supersedes NACA TN 1905 by Burrows, Braslow, and Tetervin and NACA TN 2112 by Braslow and Visconti.)

10. Diaconis, N. S., Jack, John R., and Wisniewski, Richard J.:  Boundary-Layer Transition at Mach 3.12 as Affected by Cooling and Nose Blunting.  NACA TN 3928, 1957.

16

11. Czarnecki, K. R., and Sinclair, Archibald R.: An Investigation of
    the Effects of Heat Transfer on Boundary-Layer Transition on a
    Parabolic Body of Revolution (NACA RM-10) at a Mach Number of 1.61.
    NACA Rep. 1240, 1955. (Supersedes NACA TN's 3165 and 3166.)

12. Van Driest, E. R., and Boison, J. Christopher: Experiments on
    Boundary-Layer Transition at Supersonic Speeds. Jour. Aero. Sci.,
    vol. 24, no. 12, Dec. 1957, pp. 885-899.

13. Diaconis, N. S., Wisniewski, Richard J., and Jack, John R.: Heat
    Transfer and Boundary-Layer Transition on Two Blunt Bodies at
    Mach Number 3.12. NACA TN 4099, 1957.

14. Schwartzberg, Milton A., and Braslow, Albert L.: Experimental
    Study of the Effects of Finite Surface Disturbances and Angle of
    Attack on the Laminar Boundary Layer of an NACA 64A010 Airfoil
    With Area Suction. NACA TN 2796, 1952.

15. Peterson, John B., Jr., and Horton, Elmer A.: An Investigation of
    the Effect of a Highly Favorable Pressure Gradient on Boundary-
    Layer Transition as Caused by Various Types of Roughnesses on a
    10-Foot-Diameter Hemisphere at Subsonic Speeds. NASA MEMO 2-8-59L,
    1959.

16. Jack, John R., Wisniewski, Richard J., and Diaconis, N. S.: Effects
    of Extreme Surface Cooling on Boundary-Layer Transition. NACA
    TN 4094, 1957.

17. Korkegi, Robert H.: Transition Studies and Skin-Friction Measure-
    ments on an Insulated Flat Plate at a Mach Number of 5.8. Jour.
    Aero. Sci., vol. 23, no. 2, Feb. 1956, pp. 97-107, 192.

L
2
9
6

L-296

TABLE I

DATA USED TO CALCULATE ROUGHNESS REYNOLDS NUMBER PARAMETER $\sqrt{R_{k,t}}$

| Roughness height, k, in. | Roughness station, s, in. | Critical Reynolds number per foot, R' | Critical roughness Reynolds number | $\bar{T}_w/T_o$ (approximate) |
|---|---|---|---|---|
| $10^o$ cone; $M_\infty = 1.61$ | | | | |
| 0.019 | 12.5 | $0.901 \times 10^6$ | 449.0 | Adiabatic |
| .019 | 12.5 | .769 | 382.0 | |
| .019 | 12.5 | .731 | 513.0 | } 1.289 |
| .011 | 10.4 | .974 | 278.0 | |
| .011 | 10.4 | 1.090 | 252.0 | Adiabatic |
| $10^o$ cone; $M_\infty = 2.01$ | | | | |
| 0.005 | 1.0 | $2.212 \times 10^6$ | 407.0 | |
| .010 | 2.0 | 1.206 | 480.6 | |
| .005 | 2.0 | 2.255 | 251.9 | |
| .010 | 3.0 | 1.301 | 397.4 | |
| .010 | 3.0 | 1.339 | 416.5 | } Adiabatic |
| .015 | 3.0 | 1.006 | 674.5 | |
| .023 | 5.0 | .520 | 440.5 | |
| .023 | 10.3 | .715 | 443.0 | |
| .010 | 10.4 | 1.830 | 390.1 | |
| .010 | 10.4 | 1.670 | 378.6 | |
| .010 | 10.4 | 1.670 | 398.1 | } 1.474 |
| .010 | 10.4 | 1.670 | 407.6 | |
| .010 | 10.4 | 1.768 | 289.5 | } Adiabatic |
| .019 | 12.5 | 1.174 | 537.9 | |
| .019 | 12.5 | .979 | 598.5 | } 1.474 |
| .019 | 12.5 | 1.060 | 564.6 | |
| Flat plate; $M_\infty = 1.61$ | | | | |
| 0.014* | 0.25 | $0.710 \times 10^6$ | 920.0 | } Adiabatic |
| .019 | 8.00 | .910 | 340.0 | |
| Flat plate; $M_\infty = 2.01$ | | | | |
| 0.015* | 0.25 | $0.720 \times 10^6$ | 900.0 | |
| .019* | 1.00 | .880 | 940.0 | } Adiabatic |
| .031 | 8.00 | .710 | 390.0 | |

*Denotes values for which roughness height equals boundary-layer total thickness.

Figure 1.- Sketch of hollow 10° cone used for cooling tests. All dimensions are in inches.
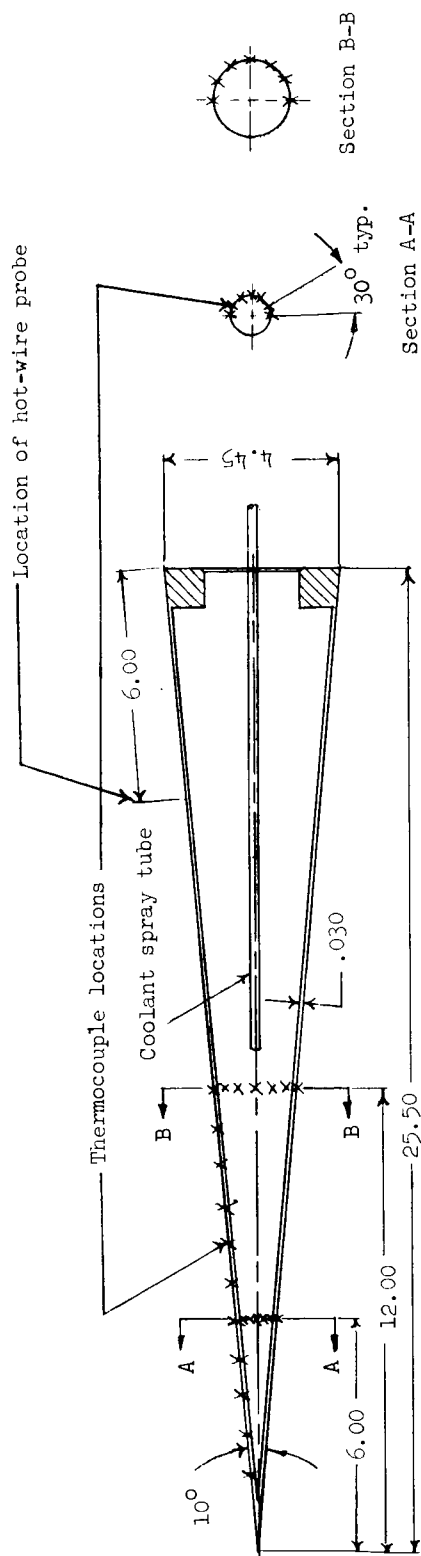
| Thermocouple locations, surface distance |
|---|
| 2.008 |
| 3.011 |
| 4.015 |
| 5.019 |
| 6.022 |
| 7.026 |
| 8.031 |
| 9.034 |
| 10.038 |
| 11.041 |
| 12.045 |

L-296

L-296
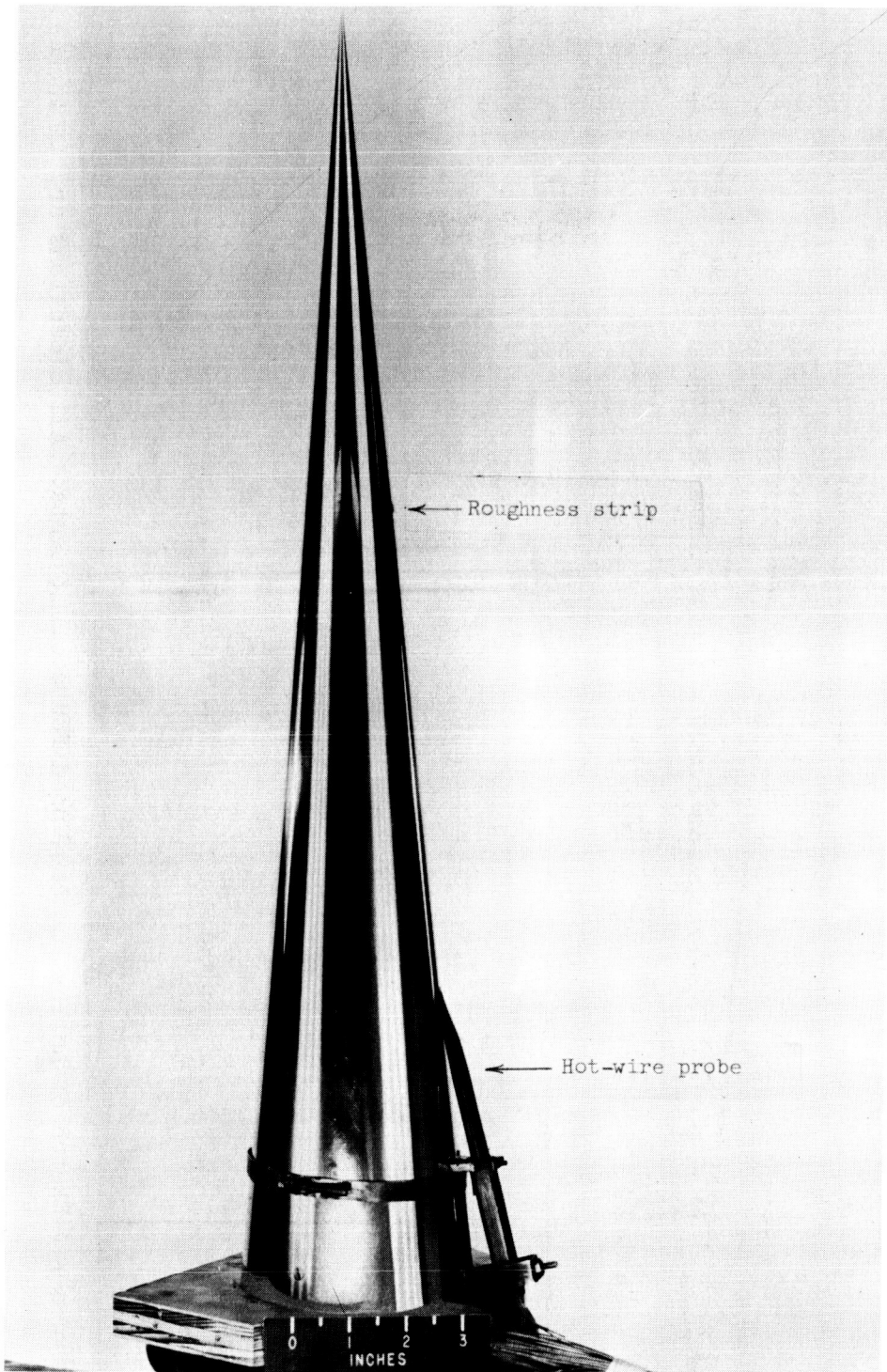


Figure 2.- Photograph of $25\frac{1}{2}$-inch-long $10^{\circ}$ cone model.    L-57-4943.1

20
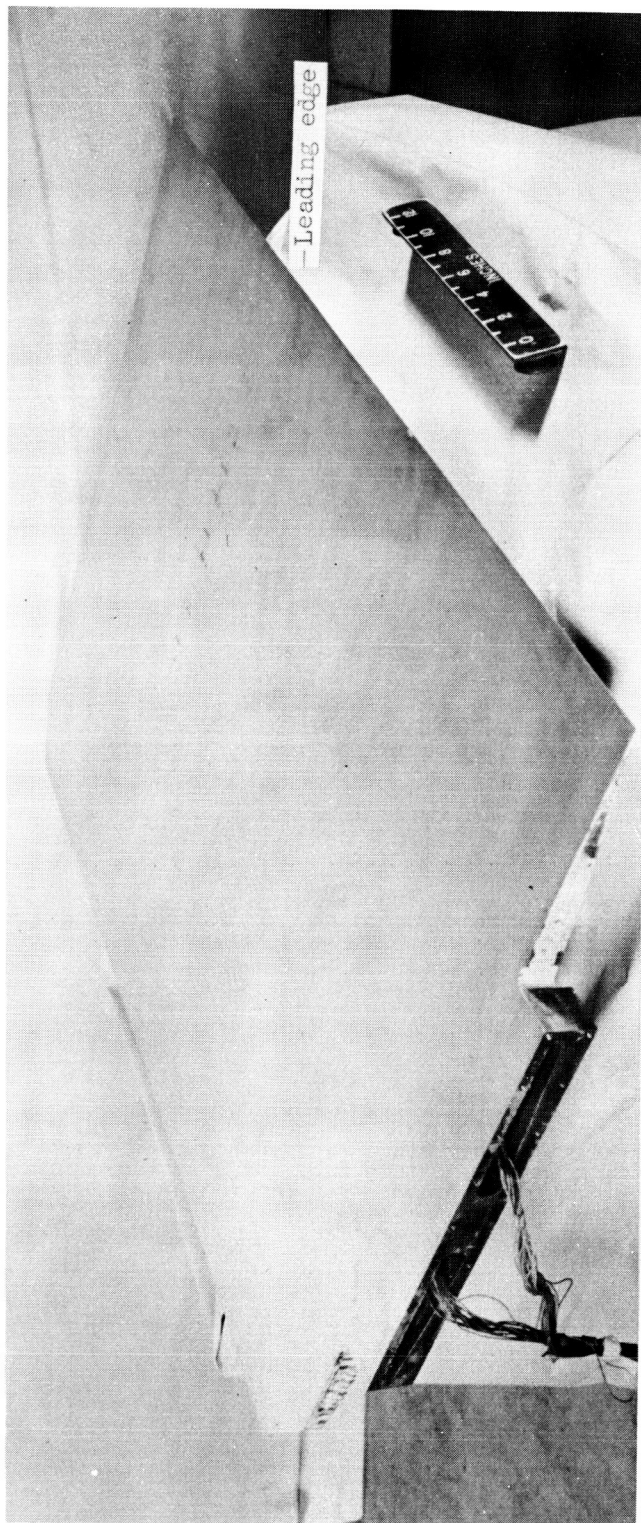


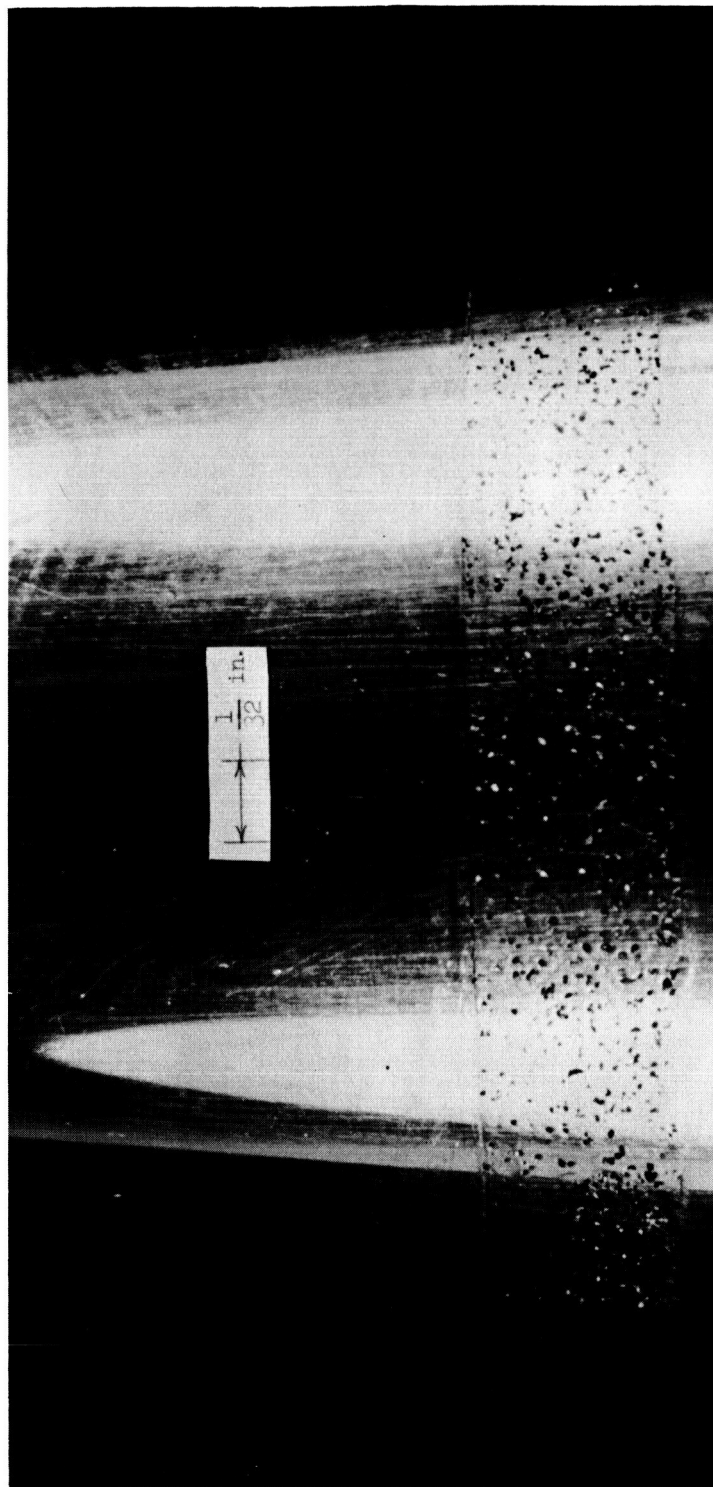Figure 3.- Photograph of 40-inch-chord flat-plate model.     L-59-1463.1

Leading edge
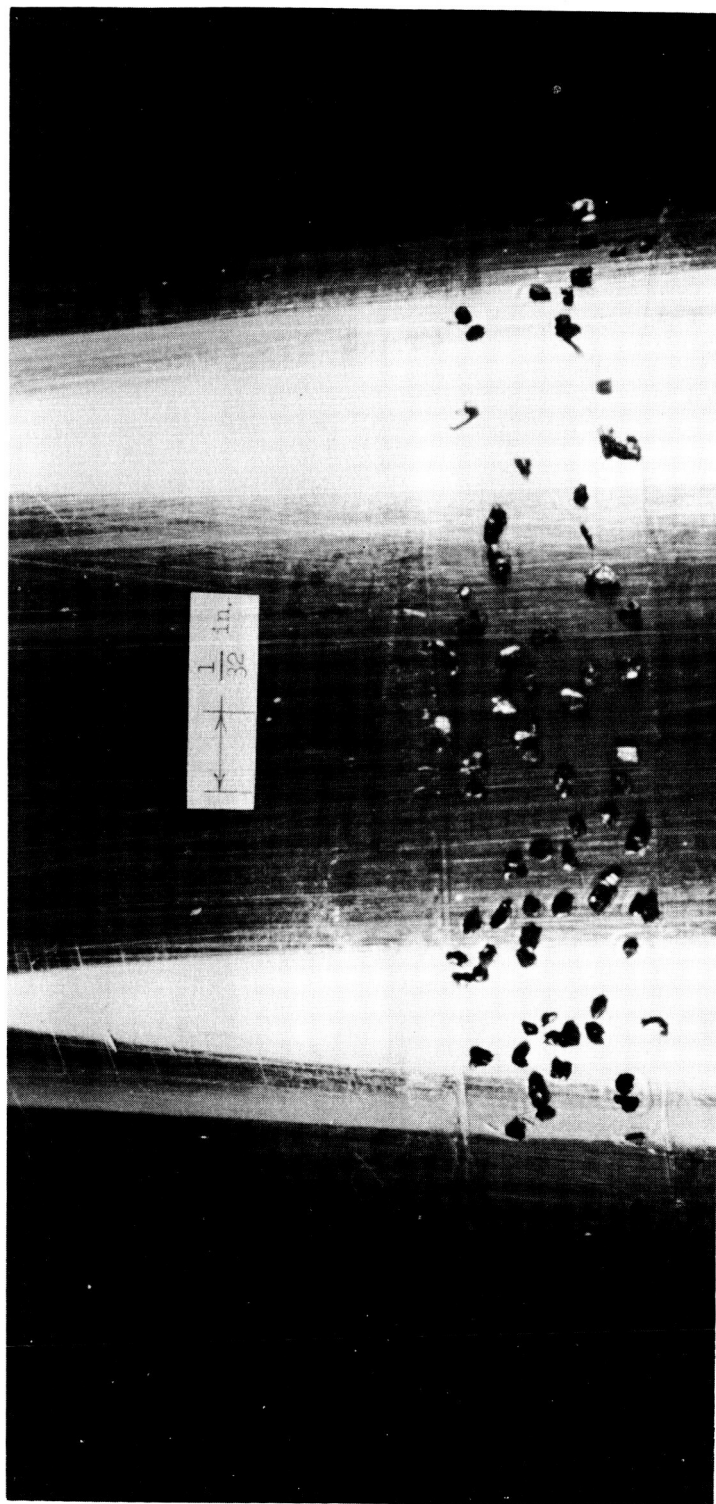
L-57-4944.1

(a) Carborundum grit No. 60.

Figure 4.- Closeup photographs of representative strips of distributed granular-type roughness.

(b) Carborundum grit No. 80.

Figure 4.- Continued.

L-57-4945.1

L-296



L-57-4946.1

(c) Carborundum grit No. 180.

Figure 4.- Concluded.

$1.00 \times 10^6$

→| |← 1/120 sec.

.98

13-1

.96

13-2

.94

.92

13-5

.90

.88

13-18

.86

.84

Reynolds number per foot, R'

L-296
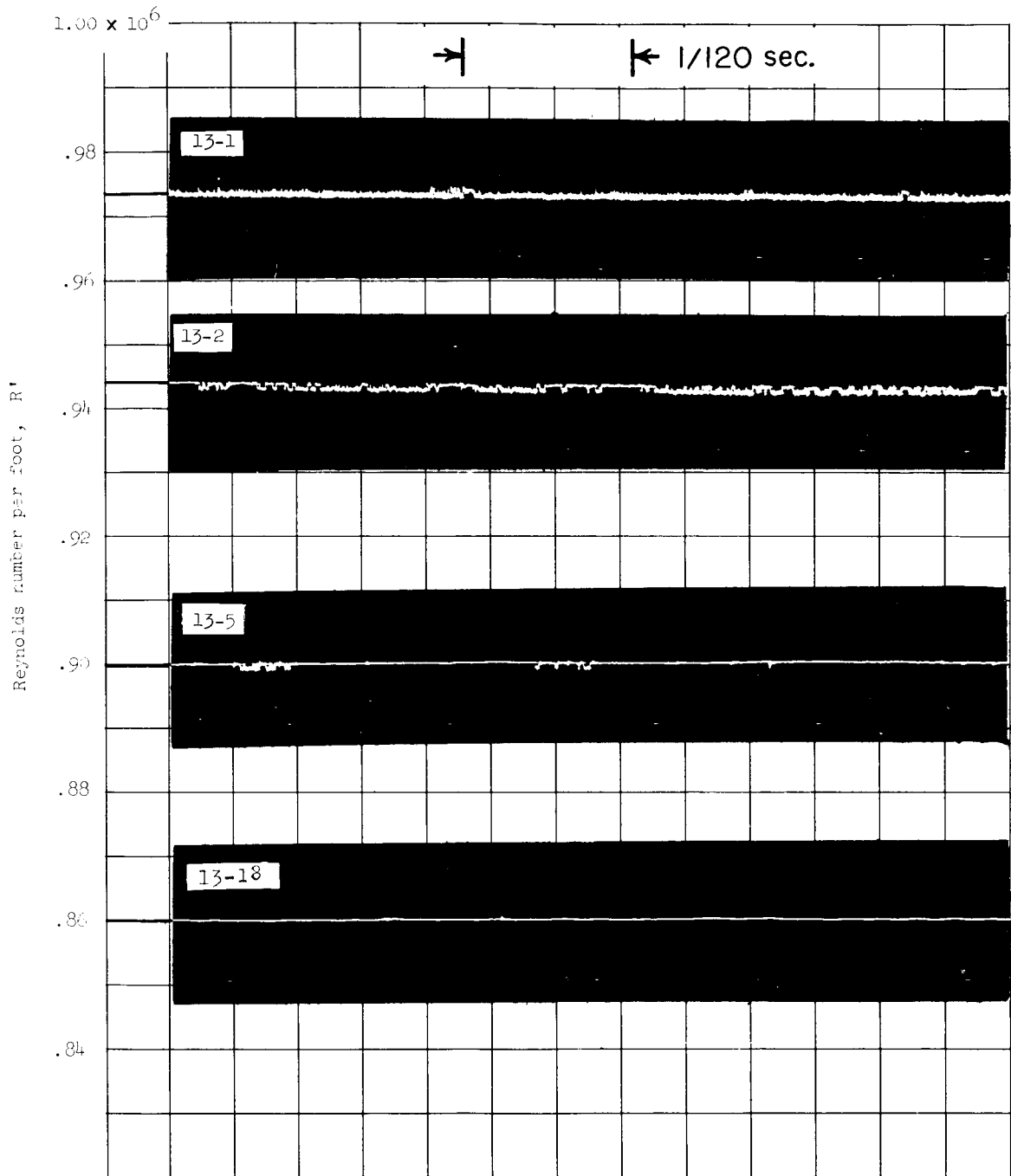
Figure 5.- Typical examples of oscillograph records of boundary-layer
velocity fluctuations through transition Reynolds number range.
0.017-inch roughness at 12.5 inches from apex of $10^\circ$ cone; $M_\infty = 1.61$.

L-296

25
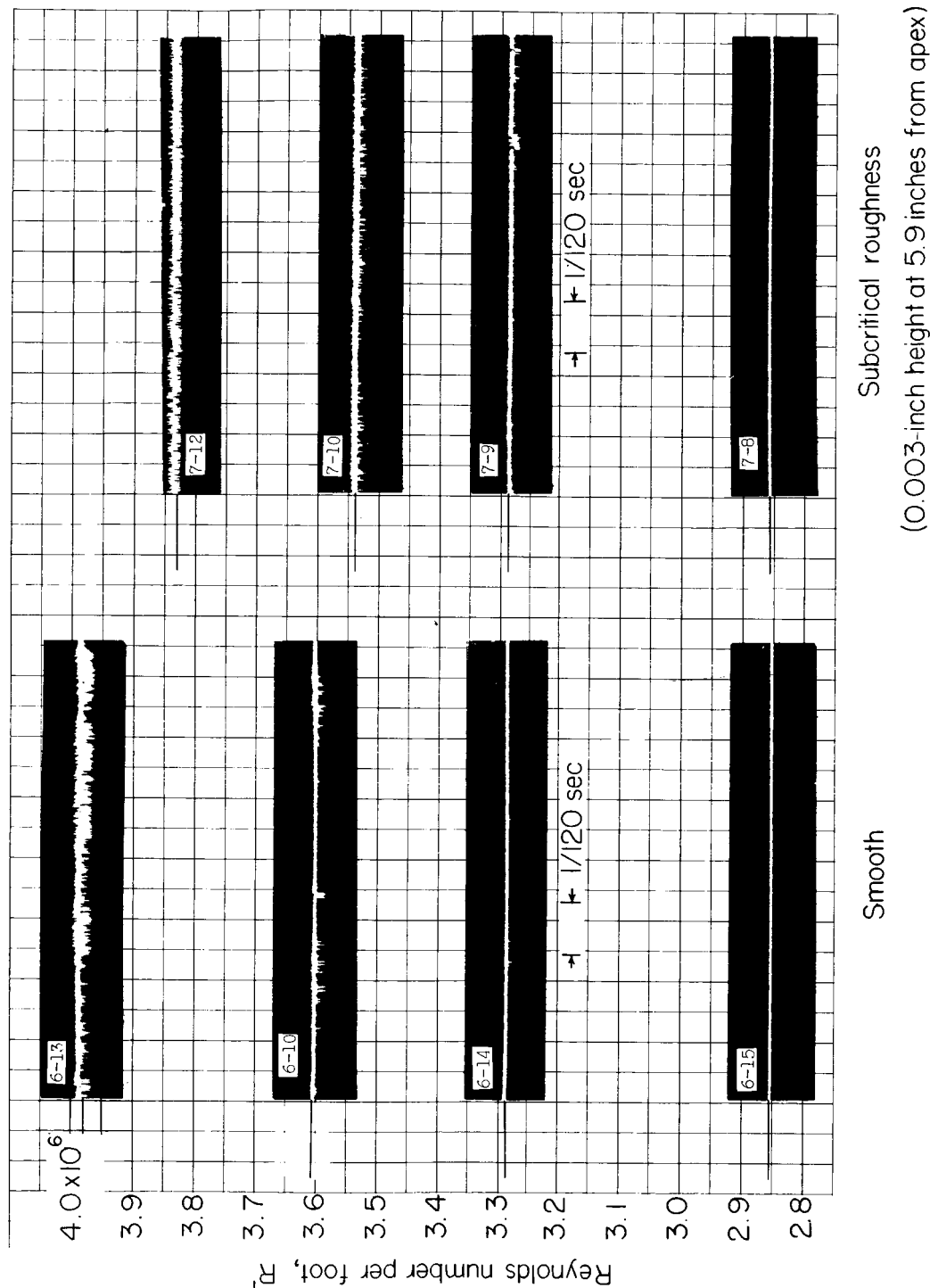


Figure 6.- Comparison of oscillograph records for smooth cone and for cone with subcritical roughness. Surface at adiabatic wall temperature; $M_\infty = 2.01$.
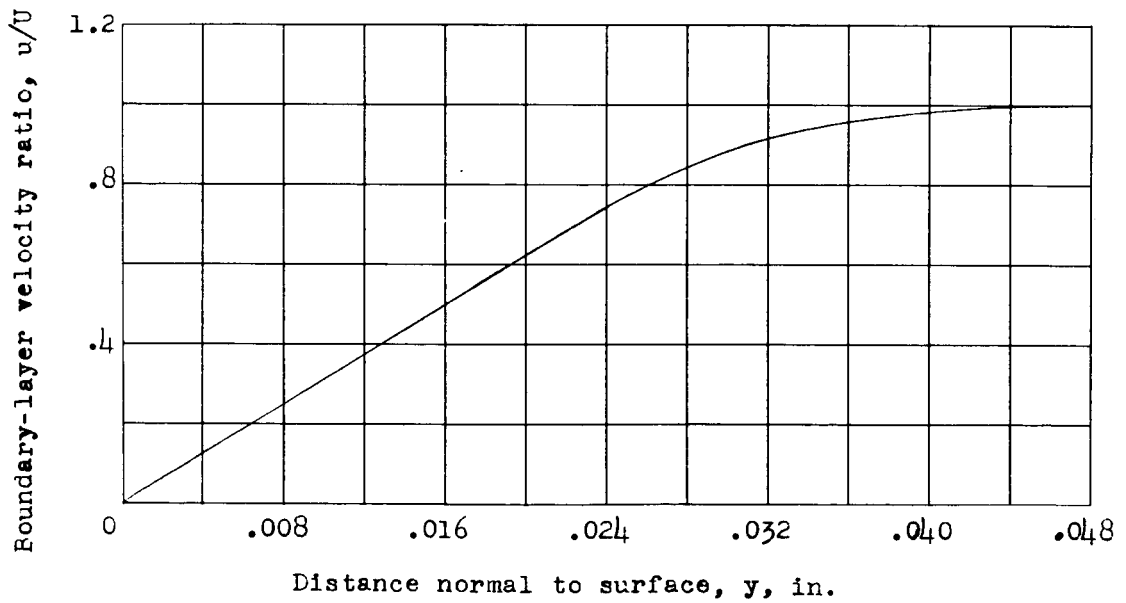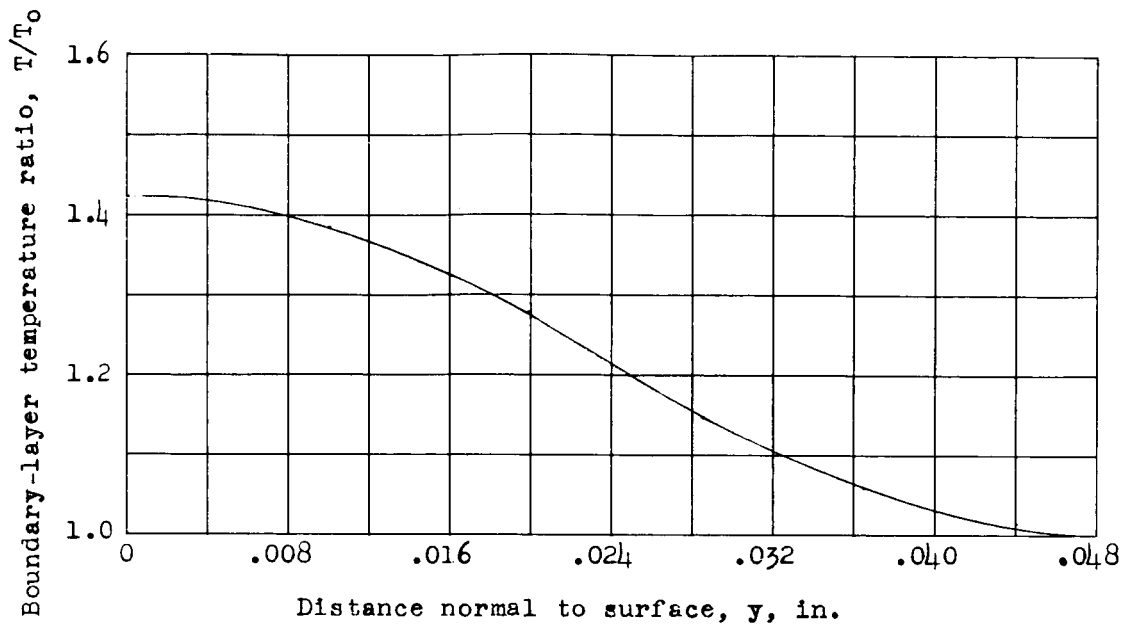
Figure 7.- Typical examples of velocity and temperature distributions through a laminar boundary layer on a $10^\circ$ cone. $M_\infty = 1.61$; $s = 12.5$ inches; $R_s = 0.799 \times 10^6$; surface at adiabatic wall temperature.
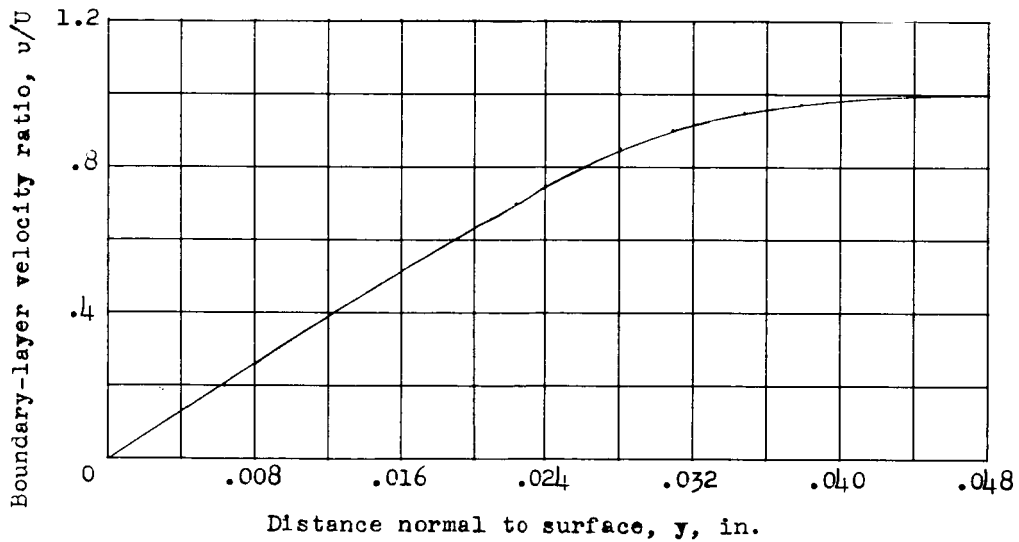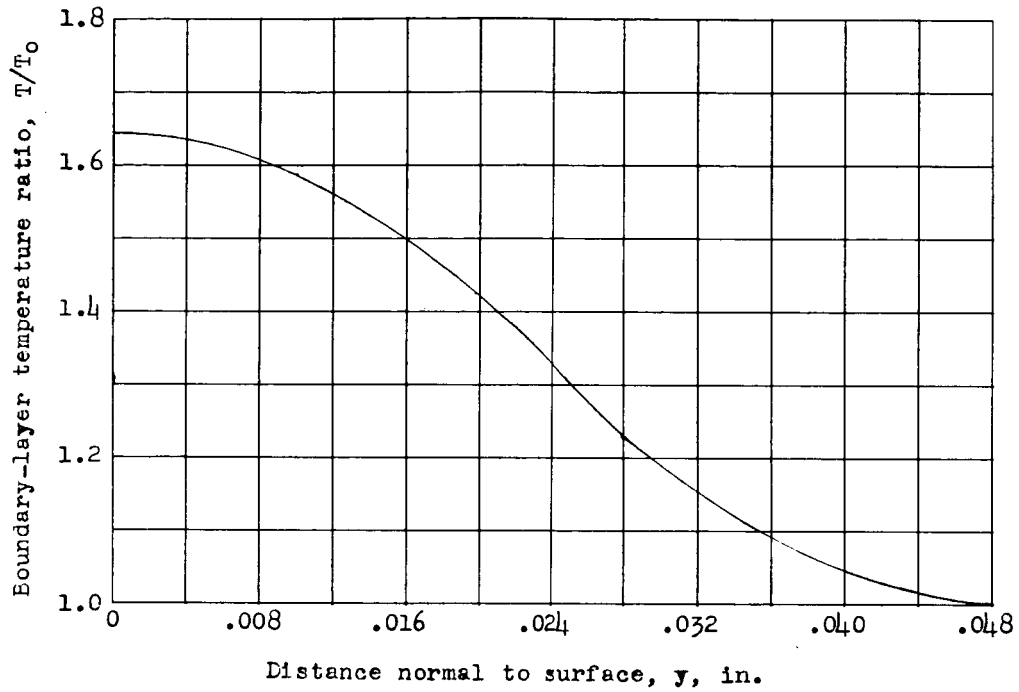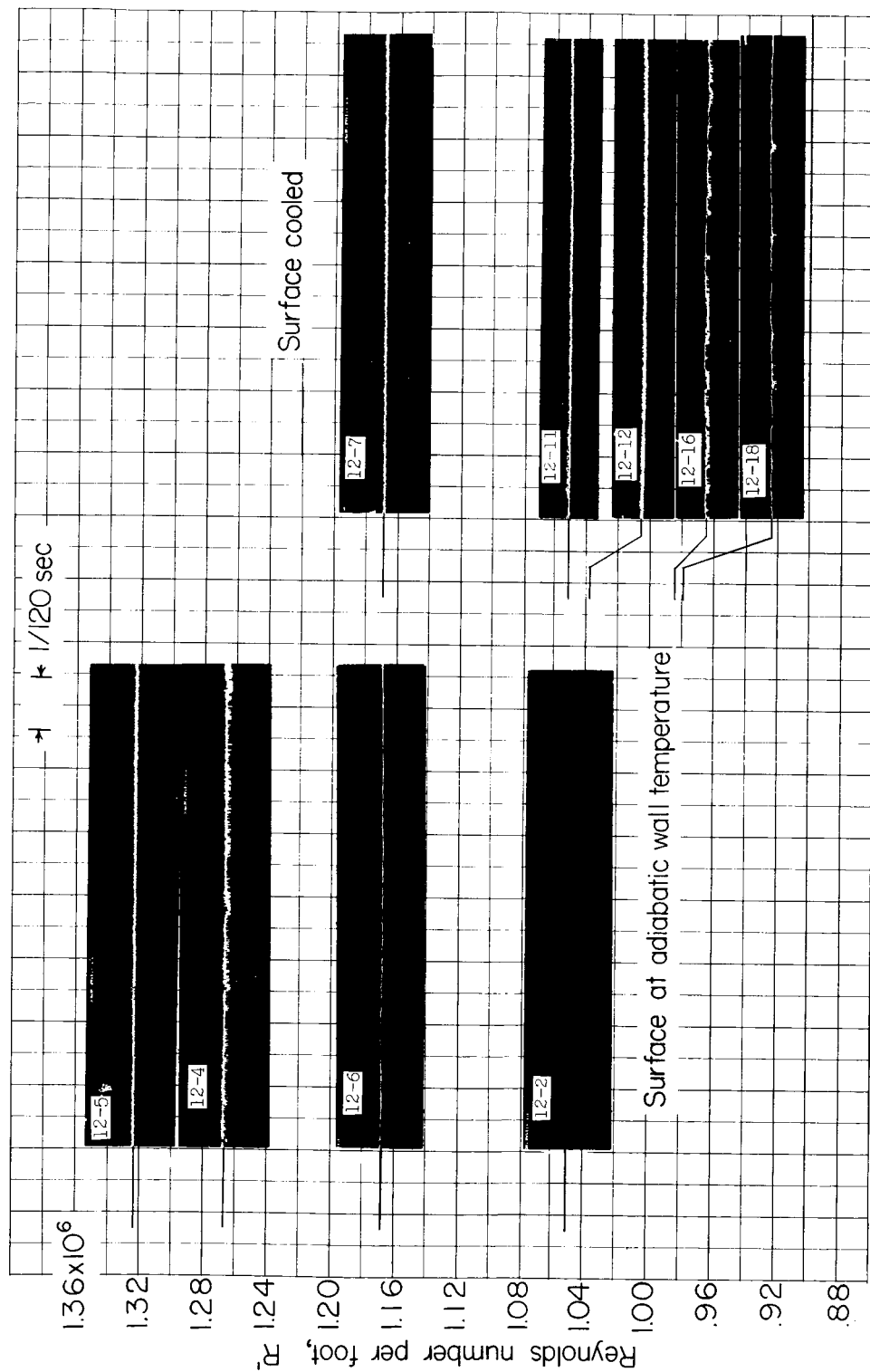
Figure 8.- Typical examples of velocity and temperature distributions through a laminar boundary layer on a 10° cone. $M_\infty = 2.01$; $s = 12.5$ inches; $R_S = 1.020 \times 10^6$; surface at adiabatic wall temperature.
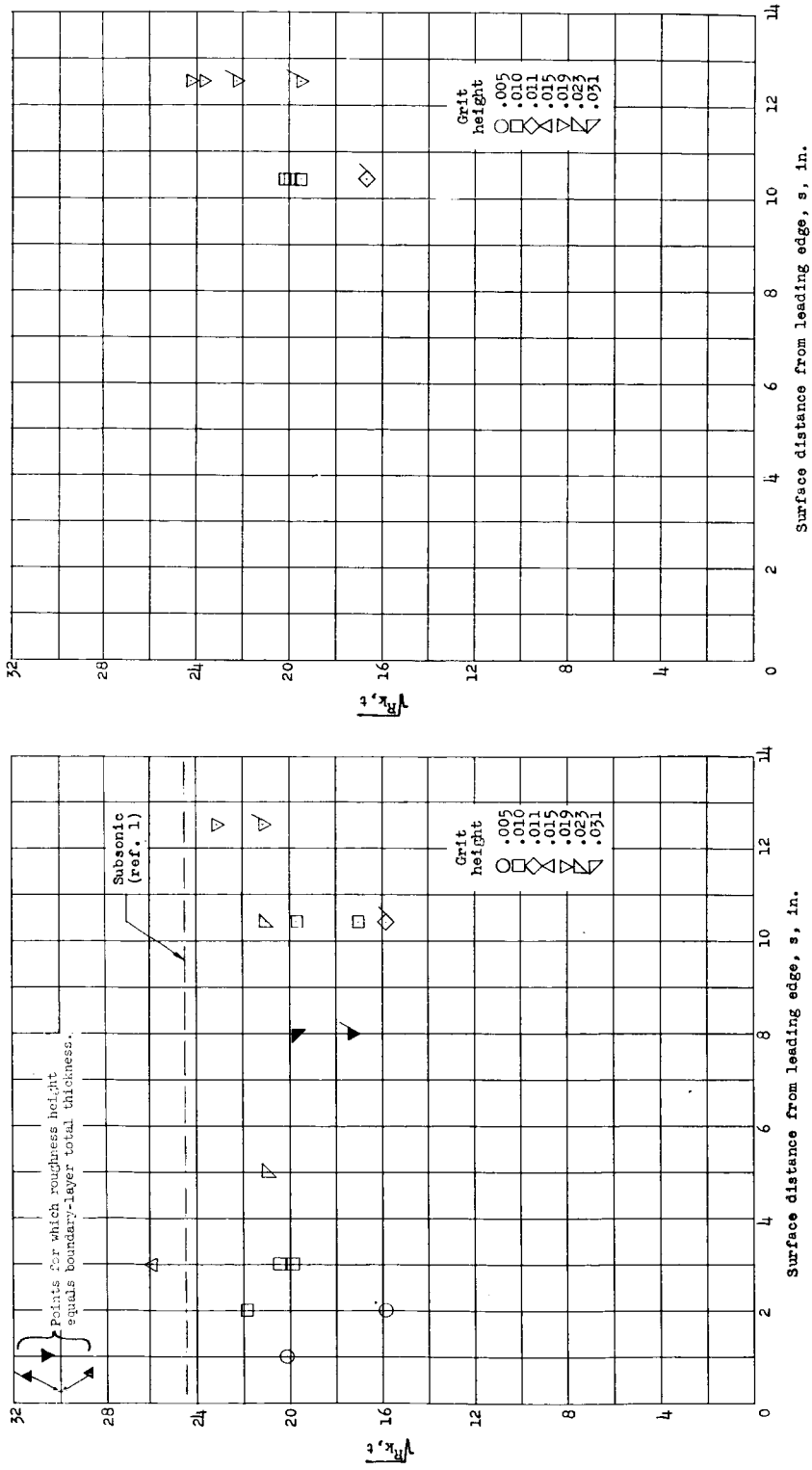
(a) Adiabatic wall.

(b) Cooled surface.

Surface distance from leading edge, s, in.

$\sqrt{R_{k,t}}$

Grit height
.005
.010
.011
.015
.019
.023
.031

Subsonic (ref. 1)

Points for which roughness height equals boundary-layer total thickness.

Figure 9.- Roughness Reynolds number for transition on 10° cone and flat-plate model as a function of roughness location for surface at adiabatic wall and cooled temperatures. Unflagged symbols denote $M_\infty = 2.01$; flagged symbols, $M_\infty = 1.61$; solid symbols, flat-plate data.
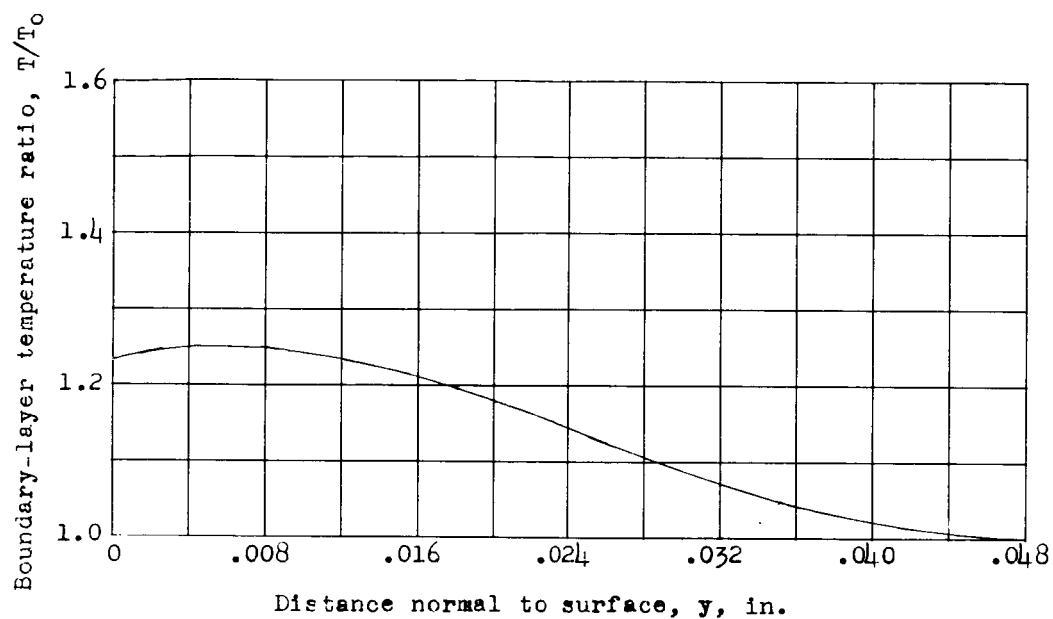
(a)  $M_\infty = 2.01$.

Figure 10.- Comparison of oscillograph records for cone surface at adiabatic wall temperature and for cone surface cooled.  0.017-inch roughness at 12.5 inches from apex.
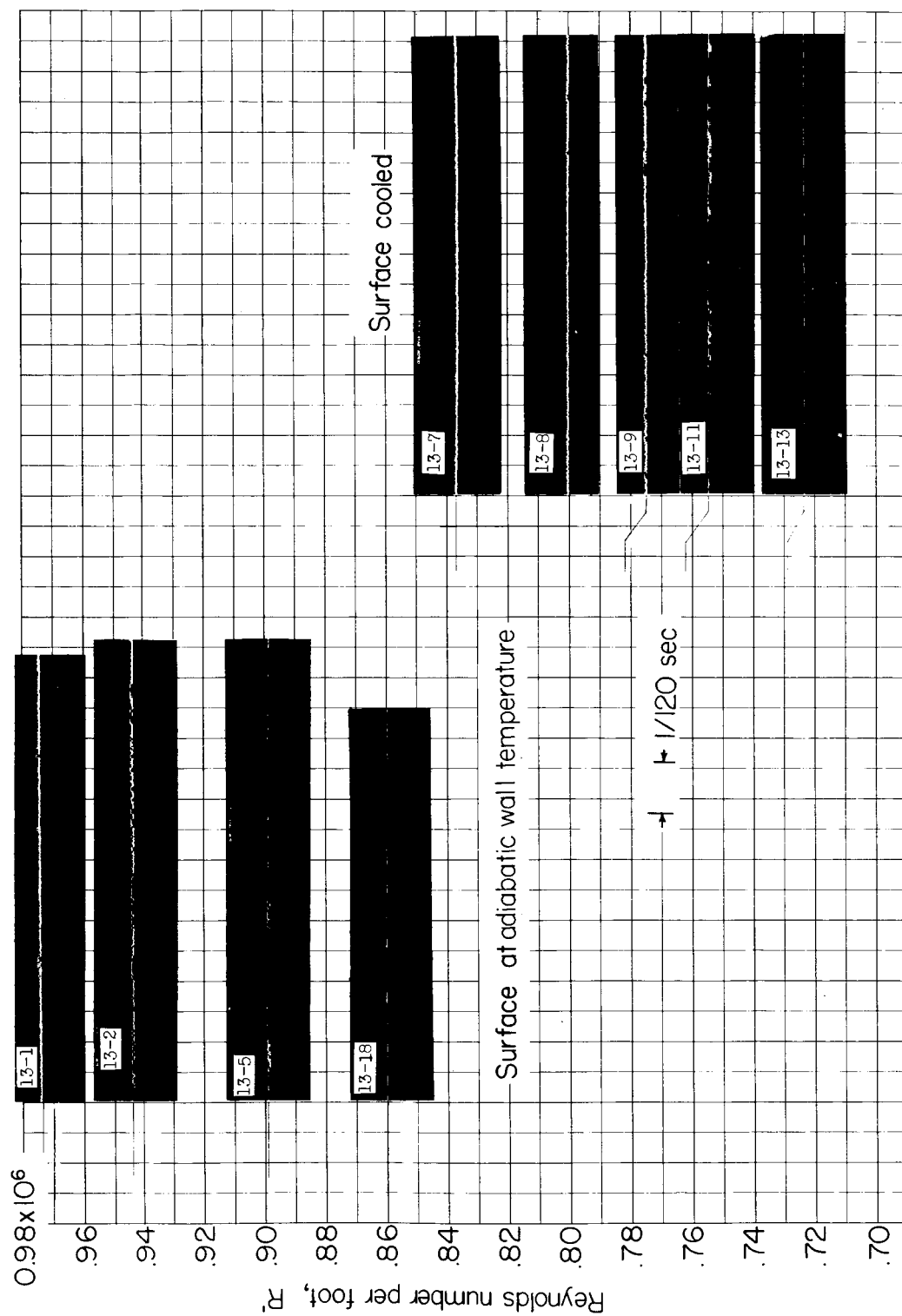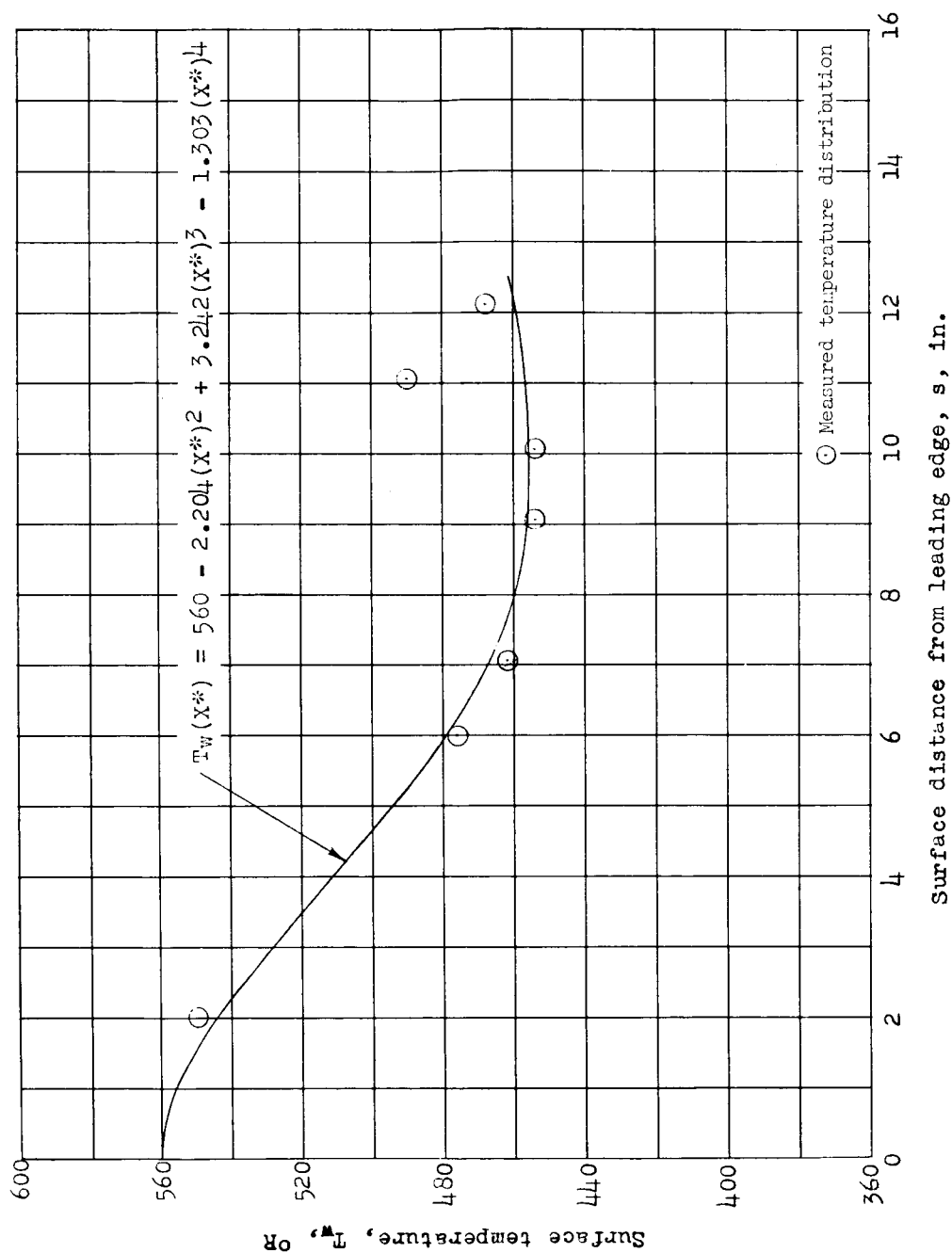
(b) $M_{\infty} = 1.61$.

Figure 10.- Concluded.

L-296

L-296
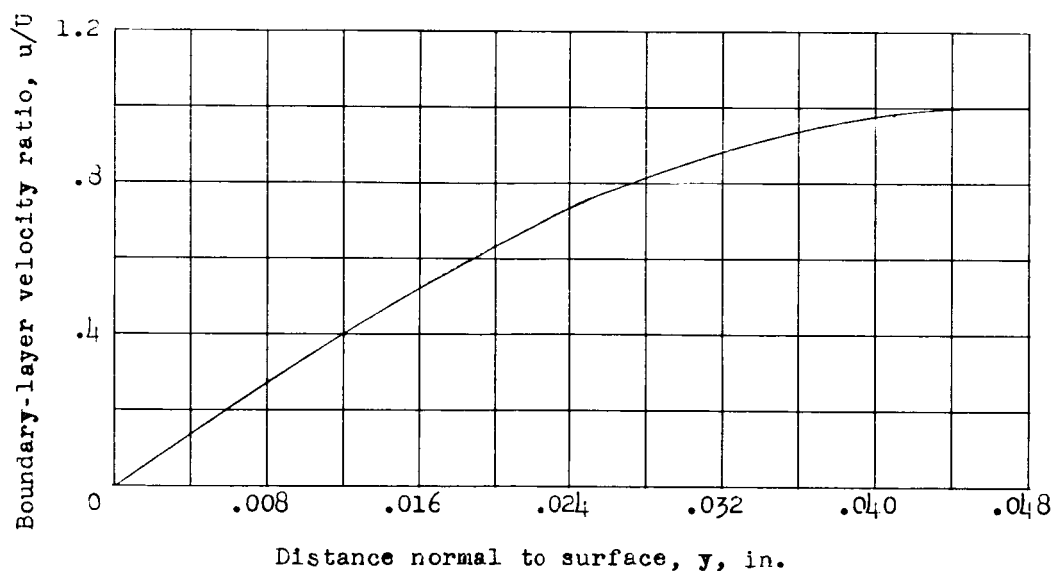


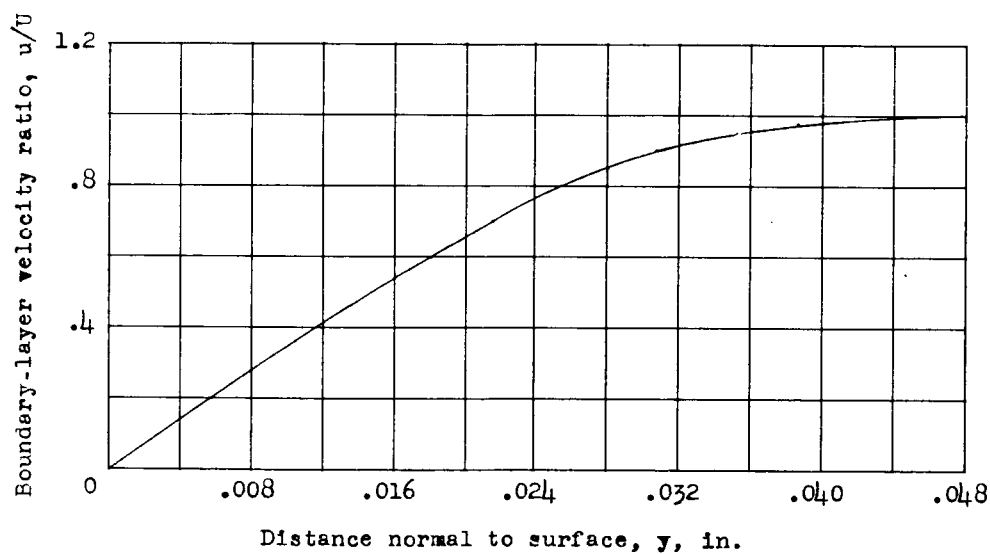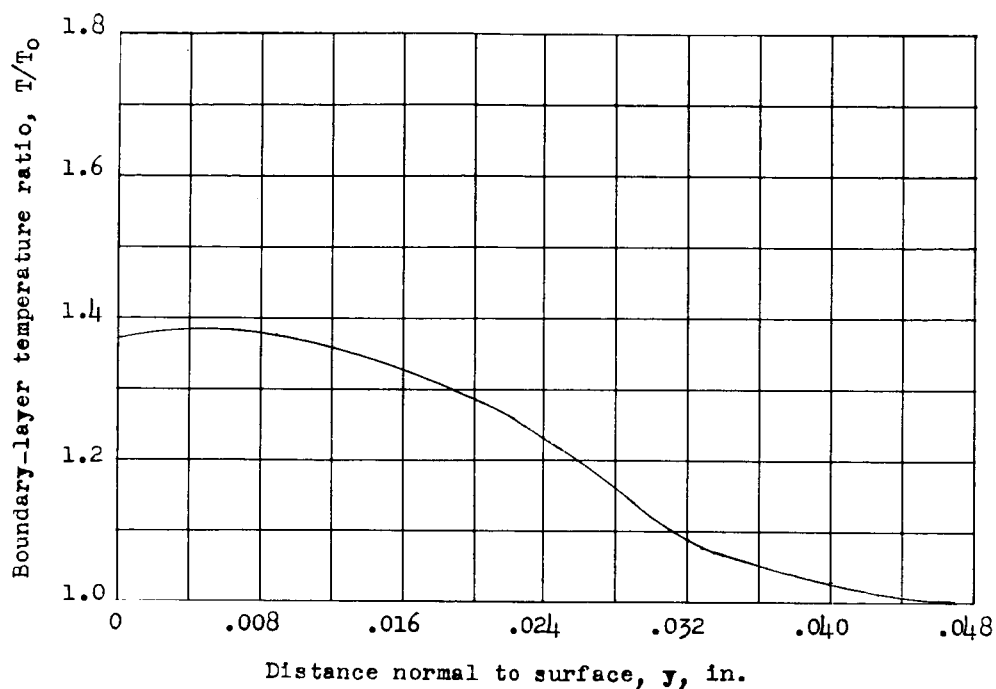(a) Boundary-layer velocity and temperature-ratio distributions.

Figure 11.- Typical velocity and temperature distributions through a
laminar boundary layer and corresponding longitudinal surface-
temperature distribution on a $10^0$ cone. $M_\infty = 1.61$; $s = 12.5$ inches;
$R_s = 0.799 \times 10^6$; surface cooled.

32



$$T_w(x^*) = 560 - 2.204(x^*)^2 + 3.242(x^*)^3 - 1.303(x^*)^4$$

⊙ Measured temperature distribution

Surface distance from leading edge, s, in.

Surface temperature, $T_w$, °R

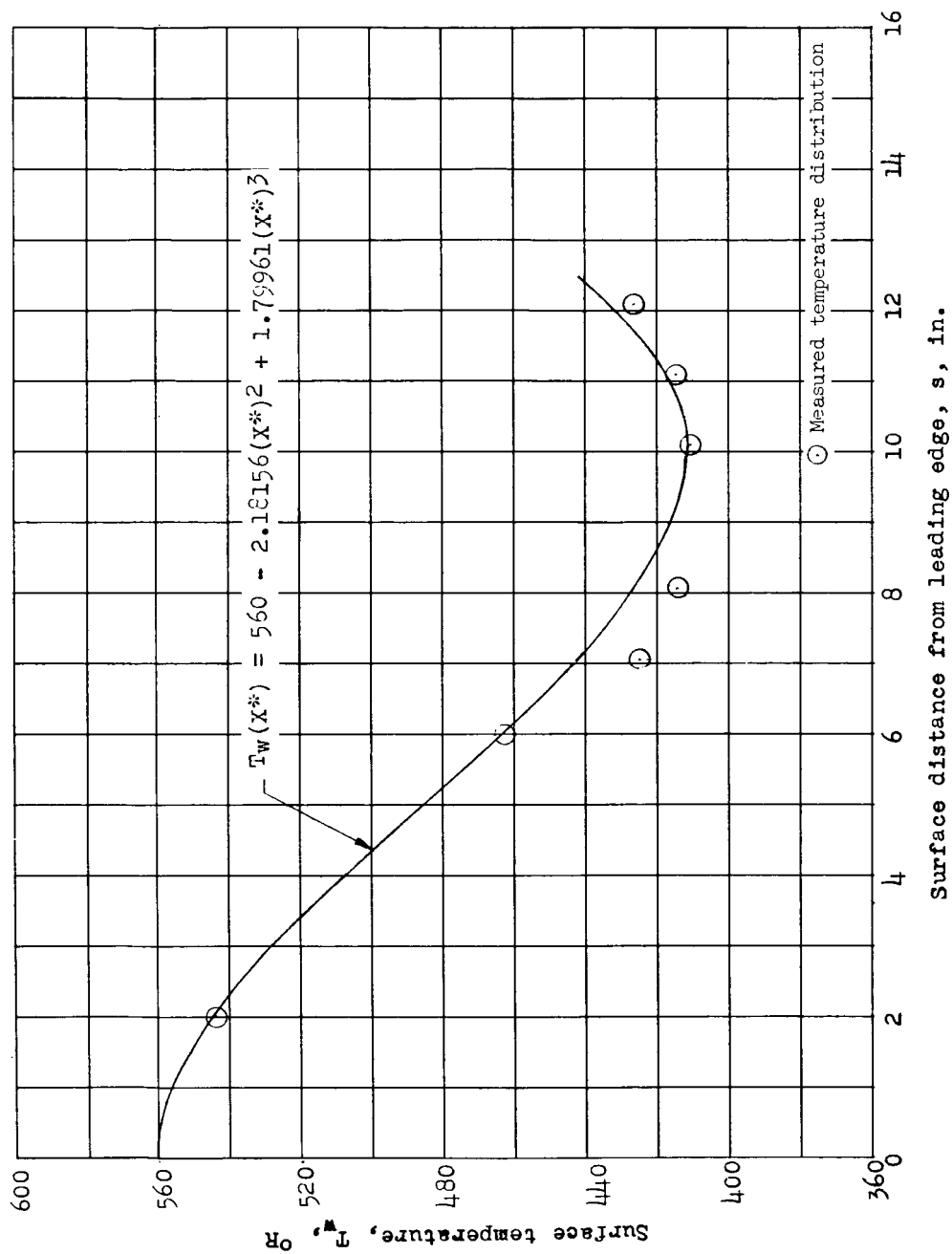(b) Longitudinal surface-temperature distribution.
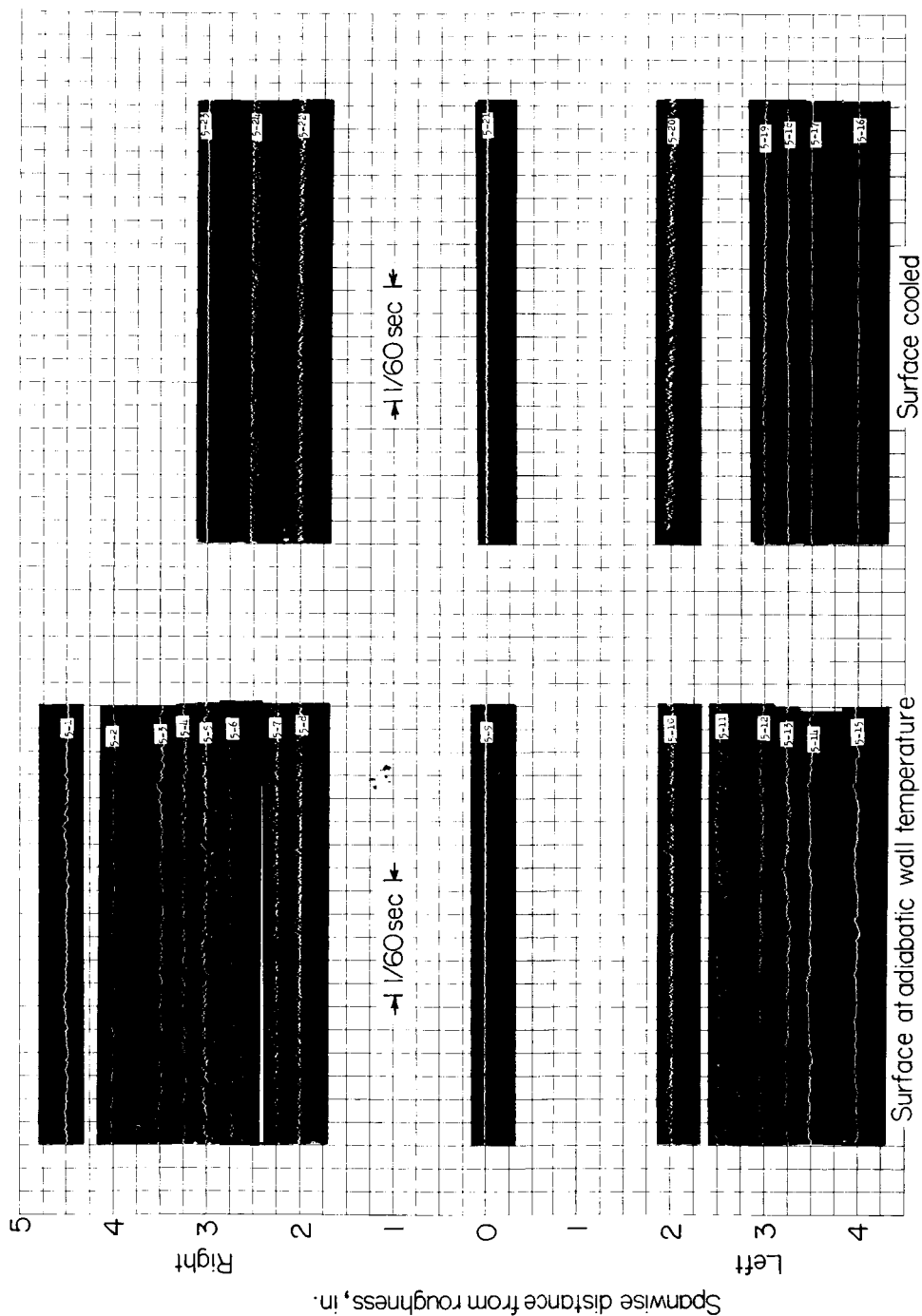
Figure 11.- Concluded.

L-296

L-296



(a) Boundary-layer velocity and temperature-ratio distributions.

Figure 12.- Typical velocity and temperature distributions through a laminar boundary layer and corresponding longitudinal surface-temperature distribution on a $10^0$ cone. $M_\infty = 2.01$; s = 12.5 inches; $R_s = 1.020 \times 10^6$; surface cooled.
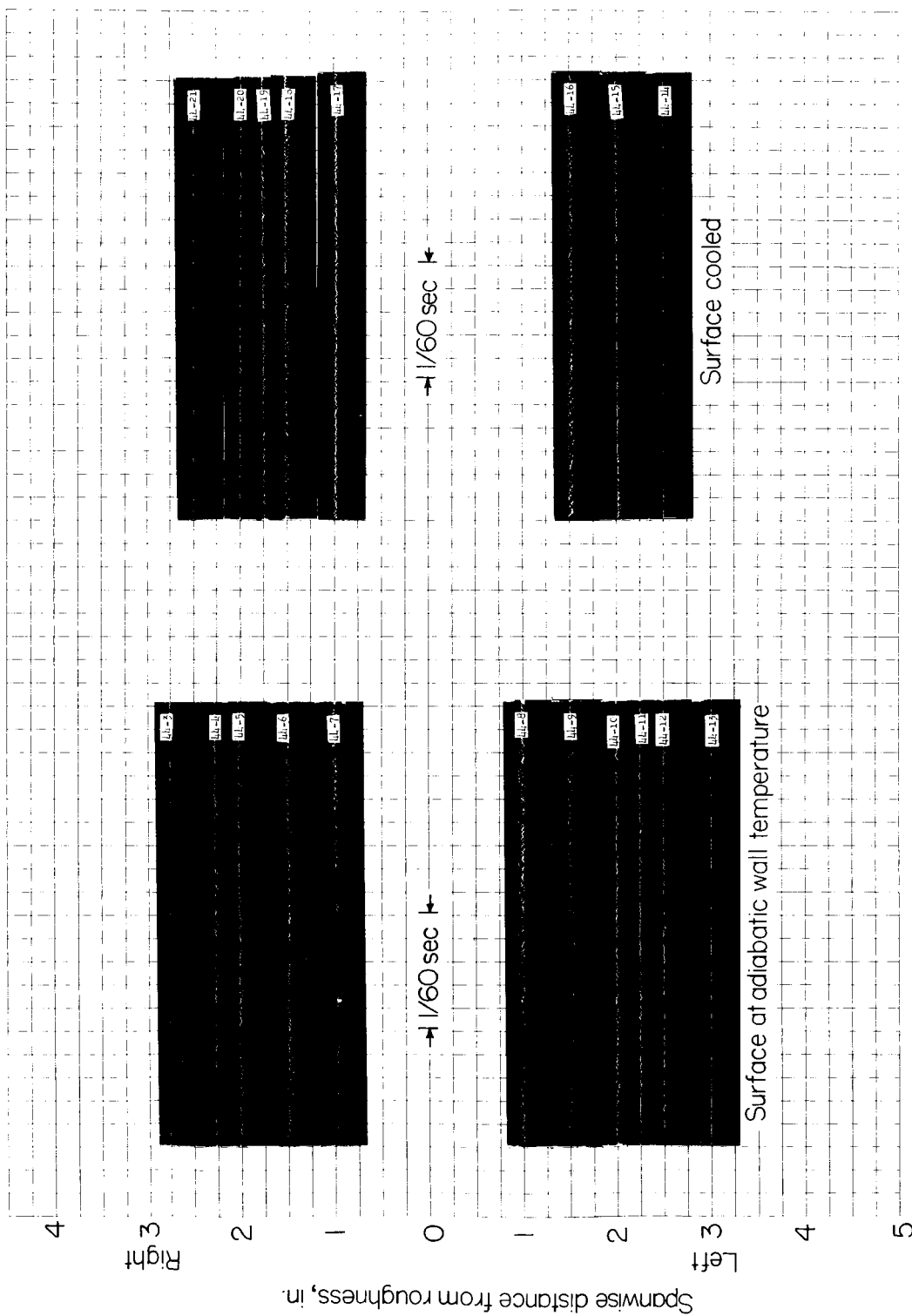
The curve is labeled with the equation:

$$T_w(X^*) = 560 - 2.18156(X^*)^2 + 1.79961(X^*)^3$$

⊙ Measured temperature distribution

Surface distance from leading edge, $s$, in.

Surface temperature, $T_w$, $^\circ R$

(b) Longitudinal surface-temperature distribution.
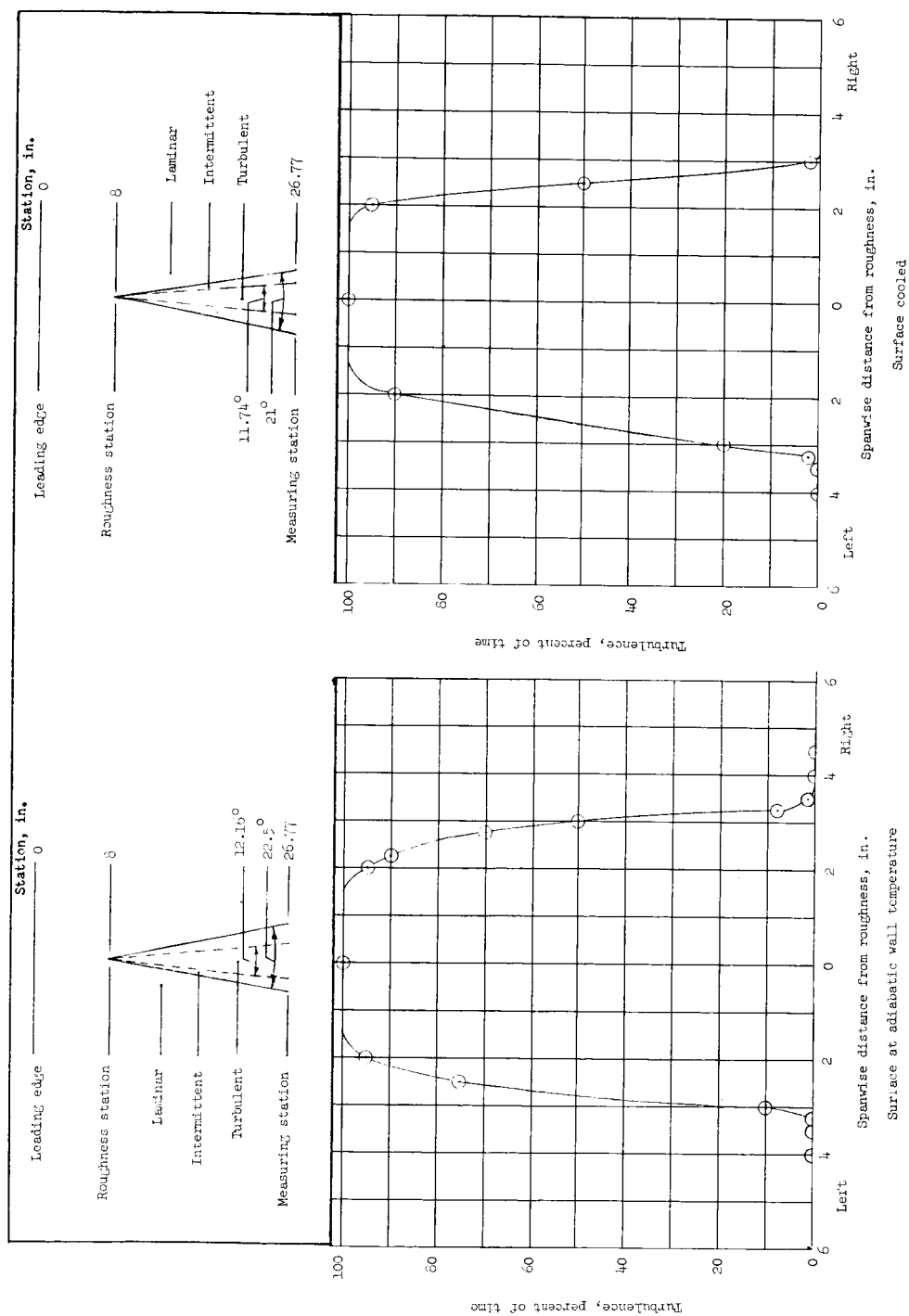
Figure 12.- Concluded.

L-296

L-296



(a) $M_\infty = M_0 = 1.61$; $k = 0.015$ inch; $s = 8$ inches.

Figure 13.- Comparison of oscillograph records at similar spanwise positions for flat-plate sur-
face at adiabatic wall temperature and cooled.

(b) $M_\infty = M_O = 2.01$; $k = 0.031$ inch; $s = 8$ inches.

Figure 13.- Concluded.

L-296

L-296

Leading edge ——————— Station, in.
                                 0

Roughness station ——————— 8

                Laminar
                Intermittent
                Turbulent

11.74°
21°

Measuring station ——————— 26.77

100

80

60

40

20

0

Turbulence, percent of time

6    4    2    0    2    4    6
Left        Spanwise distance from roughness, in.        Right

Surface cooled

Leading edge ——————— Station, in.
                                 0

Roughness station ——————— 8

                Laminar
                Intermittent
                Turbulent

12.16°
22.5°

Measuring station ——————— 26.77

100

80

60

40

20

0

Turbulence, percent of time

6    4    2    0    2    4    6
Left        Spanwise distance from roughness, in.        Right

Surface at adiabatic wall temperature

(a) $M_0 = 1.61$.

Figure 14.- Cross section of turbulence wedge 26.77 inches from leading edge showing observed percent of turbulence for several spanwise positions for flat-plate surface at adiabatic wall temperature and cooled.

(b) $M_o = 2.01$.

Figure 14.- Concluded.

L-296



(a) Flat plate; $M_\infty = M_o = 1.61$.
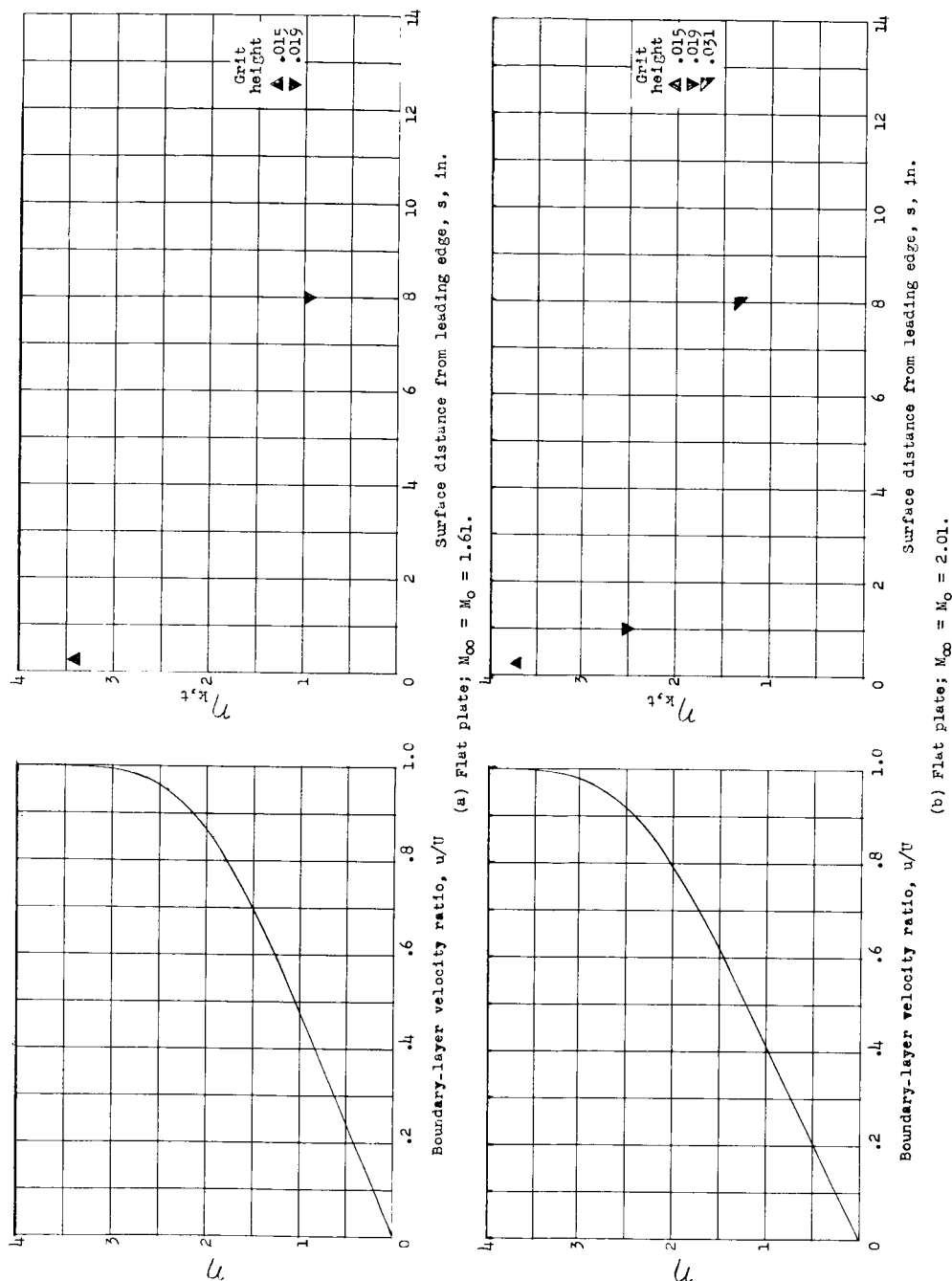
(b) Flat plate; $M_\infty = M_o = 2.01$.
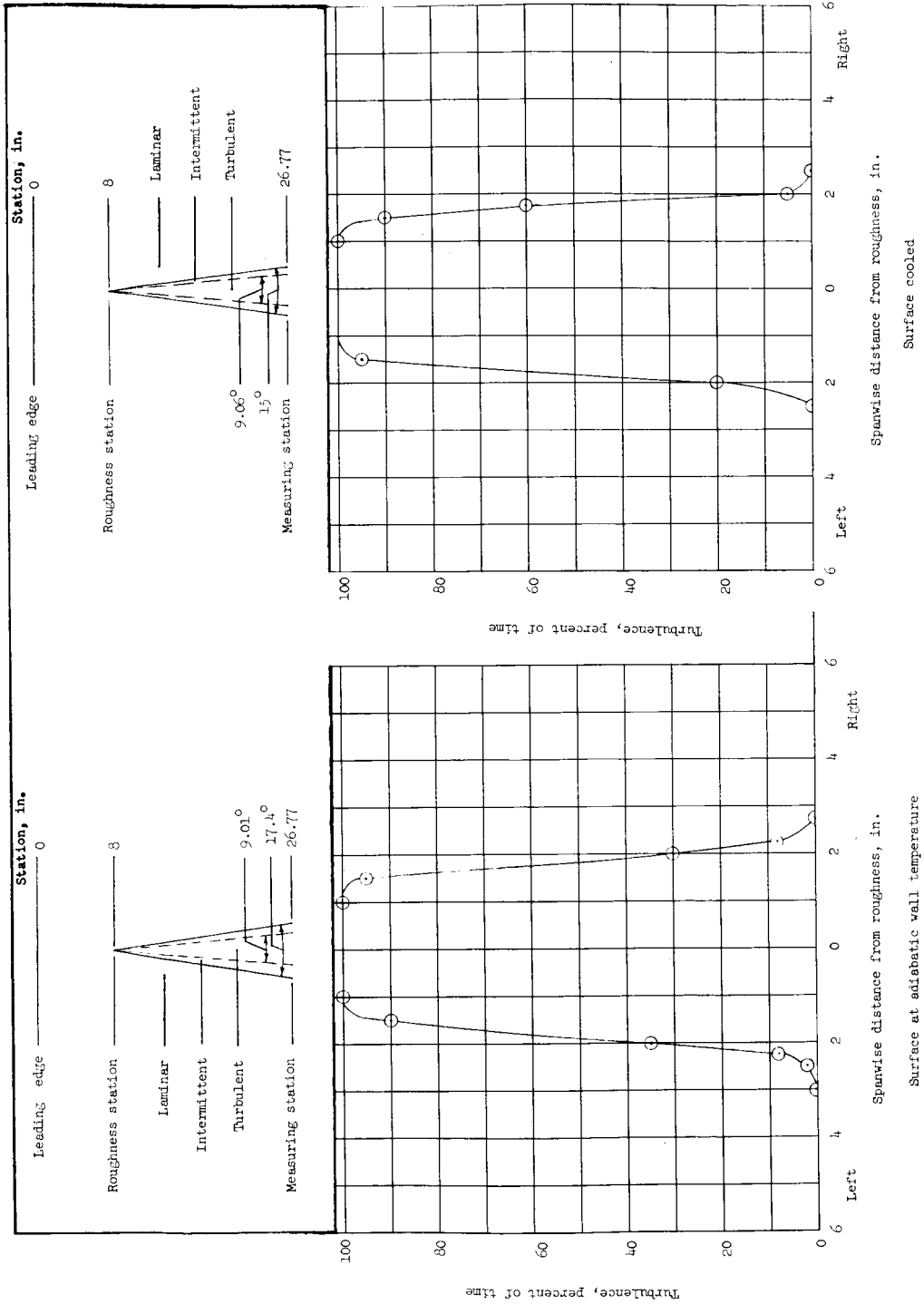
Figure 15.- Nondimensional normal distance above surface as a function of boundary-layer velocity ratio compared with nondimensional roughness height at transition as a function of surface distance to show height of roughness relative to boundary-layer thickness for several Mach numbers.
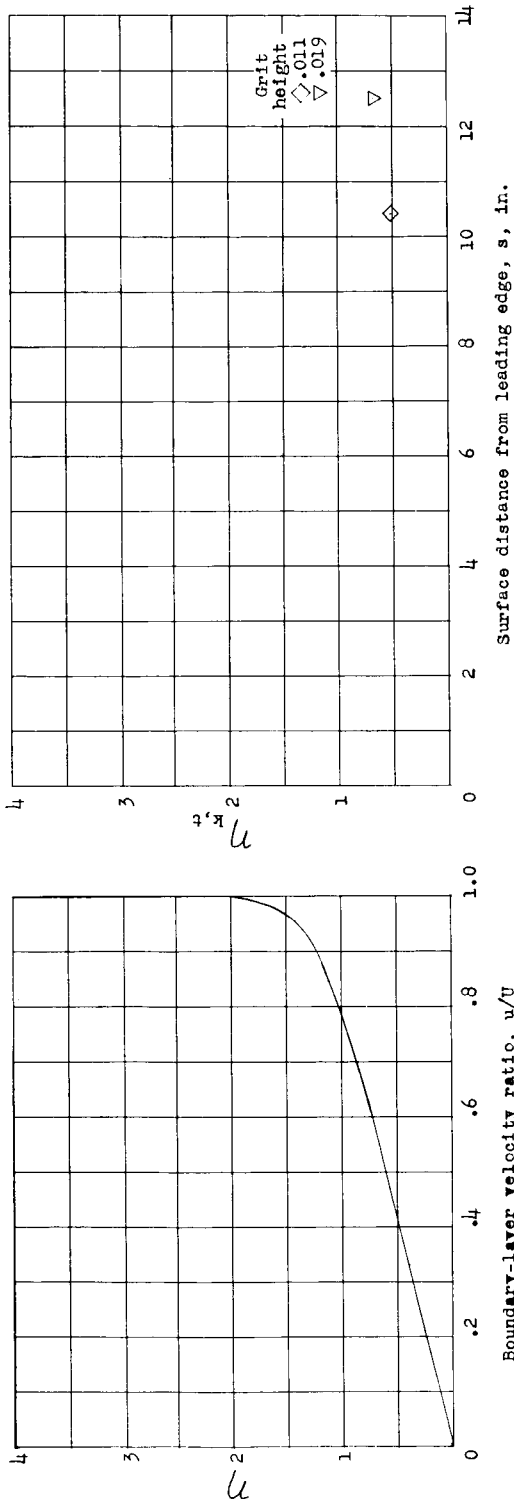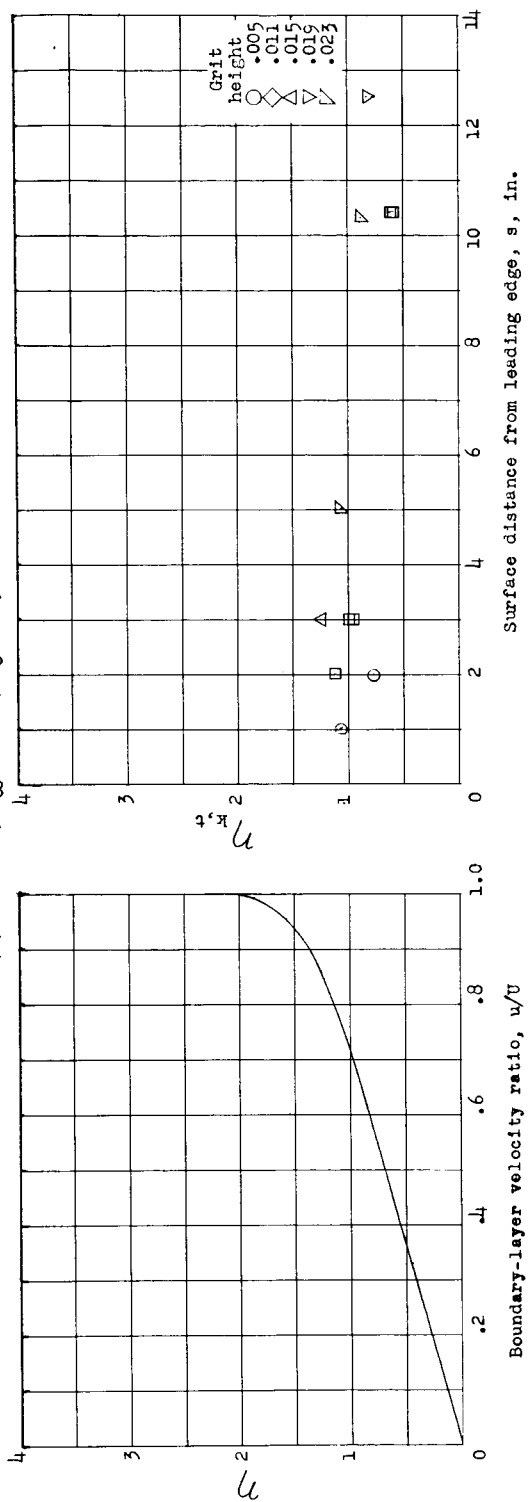
(c) 10° cone; $M_\infty = 1.61$; $M_o = 1.58$.

(d) 10° cone; $M_\infty = 2.01$; $M_o = 1.95$.

Figure 15.- Concluded.

L-296